DOUBLE-EMULSION NANOPARTICLES OF PLGA LOADED WITH RAPAMYCIN AND COLCHICINE FOR ISCHEMIA REPERFUSION INJURY TREATMENT

BY

PHOOMMAKORN THAMMAKONGTHONG 63011255

A PROJECT SUBMITTED IN PARTIAL FULFILLMENT OF THE REQUIREMENTS FOR THE DEGREE OF BACHELOR OF ENGINEERING IN BIOMEDICAL ENGINEERING

KING MONGKUT'S INSTITUTE OF TECHNOLOGY LADKRABANG

ACADEMIC YEAR 2023

SCHOOL OF ENGINEERING

KING MONGKUT'S INSTITUTE OF TECHNOLOGY LADKRABANG

PROJECT CERTIFICATE

Project Title	Double-emulsion nanoparticles of PLGA loaded with Rapamycin and Colchicine for Ischemia Reperfusion Injury Treatment
Student Name	Mr. Phoommakorn Thammakongthong Student ID. 63011255
Degree	Bachelor of Engineering in BiomedicalEngineering
Project Advisor	Signed: _____ (Assoc. Prof. Dr. Ping Ching Wu)
Project Co-Advisor	Signed: _____ (Prof. Dr. Chuchart Pintavirooj)
Committee	Signed: _____ (Asst. Prof. Dr. Treesukon Treebupachatsakul)
Committee	Signed: _____ (Asst. Prof. Dr. Kasama Srirussamee)
Committee	Signed: _____ (Asst. Prof. Dr. May Phu Paing)
Head of Department	Signed: _____ (Assoc. Prof. Dr. Sarinporn Visitsattapong)

Project Title	Double-emulsion nanoparticles of PLGA loaded with Rapamycin and Colchicine for Ischemia Reperfusion Injury treatment
Student Name	Mr. Phoommakorn Thammakongthong
Degree	Bachelor of Engineering in BiomedicalEngineering
Project Advisor	Assoc. Prof. Dr. Ping Ching Wu
Project Co-Advisor	Assoc. Prof. Dr. Chuchart Pintavirooj
Academic Years	2023

ABSTRACT

This project presents the process of creating a double emulsion nanoparticle of PLGA loaded with rapamycin and colchicine purpose for a new therapeutic way for ischemia reperfusion injury treatment. Rapamycin and Colchicine exhibit properties in the treatment of ischemia-reperfusion injury. Rapamycin demonstrates its efficacy by inhibiting the mTOR signaling pathway, thereby inhibiting autophagy. Colchicine operates by inhibiting the formation of tubulin, consequently inhibiting microtubule formation. This mechanism is beneficial to the cardiovascular system, effectively inhibiting cell proliferation. The use of PLGA to encapsulate drugs with both hydrophilic and hydrophobic properties in nanoscale sizes is aimed to creating water-oil-water double emulsion nanoparticle droplets. Observe the percent encapsulation efficiency and percent drug loading using UV-VIS of the particle's characterization method using zeta potential to determine the surface charge of the particles and Dynamic Light Scattering (DLS) to measuring the size and the size distribution of the nanoparticle synthesized.

ACKNOWLEDGEMENTS

I would like to take this opportunity to express my gratitude to all the individuals who contributed to the completion of this project. First and foremost, I want to express my appreciation to my project advisor, Associate Prof. Dr. Ping Ching Wu for his warm welcome, expert guidance and unwavering support during this project. I also wish to recognize the entire lab members for their invaluable assistance and guidance, both in the laboratory and in adapting to life in a foreign environment. Their camaraderie and support have made this journey more enjoyable and rewarding.

Last but not least, I want to convey my deep gratitude to my co-advisor, Associate Prof. Dr. Chuchart Pintavirooj for providing me with a remarkable opportunity. Without his generous support and invaluable insights, this project would not have been possible.

Phoommakorn Thammakongthong

TABLE OF CONTENTS

LIST OF FIGURES

LIST OF TABLES

LIST OF SYMBOLS/ABBREVIATIONS

Symbols/Abbreviations	Terms
PLGA	Poly(lactic-co-glycolic acid)
CVD	Cardiovascular Disease
NF-κB	Nuclear Factor-kappa B
HIF	Hypoxia Inducible Factor
TLRs	Toll-Like Receptors
NOX	NADPH oxidase
iNOS	Nitric Oxidase synthases
SEM	Scanning Electron Microscope
FDA	Food & Drug Administration
mTOR	Mammalian Target of Rapamycin
DMSO	Dimethyl Sulfoxide
ER	Endoplasmic Reticulum
AMPK	AMP-activated protein kinase
4E-PB1	4E-binding protein 1
PCG-1α	Peroxisome Proliferator-Activated Receptor Gamma Coactivator 1-alpha
HIF-1α	Hypoxia-Inducible Factor 1-alpha
mg/ml	milligrams per milliliter
AGC	Protein kinase A,G,C
PKC	Protein kinase C
PI3K	Phosphoinositide 3-kinase

CHAPTER 1

INTRODUCTION

This chapter introduces the background and information of this project. It is about the ischemia-reperfusion injury model, which is one of the cardiovascular diseases. To achieve the goal of reducing the incidence, new potential therapeutic inventions need to be introduced. Double-emulsion nanoparticle techniques that produce double-layered liquid droplets by using the poly(lactic-co-glycolic acid) (PLGA) as an emulsifier loaded with Rapamycin and Colchicine which is a medicine that gives an ischemia-reperfusion injury treatment. The research objectives are followed by the hypothesis and research scope [1].

1.1 Background and significance of the study

Cardiovascular diseases (CVD) are leading global causes of death, comprising around 30% of worldwide fatalities, with over 17 million deaths annually. The increasing lifespan and prevalence of risk factors for cardiovascular diseases, such as obesity, diabetes, and metabolic syndrome in young individuals, are directly linked to the growing incidence of CVD over the past two to three decades. There has been a significant effort to comprehend the molecular-level processes associated with ischemic injury development. This review aims to summarize the current understanding of the molecular-level mechanisms underlying the development of damage from ischemia, explore innovative treatment approaches with the potential to reduce acute myocardial injury, and investigate post-ischemic cardiac remodeling. This report provides an overview of the causes of ischemia, the molecular-level mechanisms responsible for ischemic myocardial damage and introduces novel therapeutic strategies for mitigating acute myocardial injury and addressing post-ischemic cardiac remodeling [2].

Double-emulsion nanoparticles represent a liquid dispersion system where droplets of one dispersed liquid are further dispersed within another liquid, resulting in double-layered liquid droplets, commonly referred to as water in oil in water (W/O/W) emulsion. This system facilitates the encapsulation of both hydrophilic and hydrophobic compounds. In this process, the dissolving polymer is PLGA with the first drug intended for encapsulation in this organic phase. Followed by the

emulsification of a second drug forming a water phase. This results in the formation of distinct layers within the same nanoparticle [3]. The potential application of double-emulsion nanoparticles lies in introducing a novel treatment approach that allows for the co-delivery of multiple drugs with distinct properties, particularly beneficial for combination therapy. Co-delivering two drugs with complementary mechanisms of action in a double emulsion can enhance therapeutic outcomes by providing controlled release of multiple agents at the desired time and location of drug action. Moreover, double-emulsion nanoparticles safeguard both hydrophilic and hydrophobic drugs from degradation, preventing premature drug release before reaching the target [4]. This system also has the potential to minimize side effects by delivering drugs directly to the target site through sustained release . Colchicine operates by inhibiting the formation of tubulin, consequently inhibiting microtubule formation.

Rapamycin and Colchicine are two drugs that have a therapeutic effect for ischemia reperfusion injury treatment including mTOR inhibitor properties of Rapamycin that lead to inhibiting autophagy that potentially restore balance and inhibit the inflammation of the cells [5], inhibition of microtubule polymerization cause by Colchicine operates by inhibiting the formation of tubulin, further inhibit the neutrophils activities of anti-inflammatory effects, consequently inhibiting endothelial cells proliferation. Additionally, working together with Rapamycin and Colchicine enhances therapeutic effect for ischemia reperfusion injury treatment [6].

1.2 Objectives

1.2.1. To understand the mechanism of the cause of ischemia reperfusion injury.

1.2.2. To encapsulate Rapamycin and Colchicine within one nanoparticle.

1.2.3. To enhance the therapeutic of the drug by creating a double emulsion nanoparticle of PLGA loaded with Rapamycin and Colchicine.

1.2.4. To prevent the patient from ischemia reperfusion injury.

1.3 Scope of the study

This research is based on the knowledge of understanding the mechanism of reperfusion injury and double-emulsion nanoparticles for Ischemia reperfusion injury treatment. This report will focus on how to create a double emulsion nanoparticle of

PLGA loaded with Rapamycin and Colchicine. While understanding the mechanisms and properties of Rapamycin and Colchicine.

1.3 Report outline

The following contents of this report is organized as follows:

Chapter 2 reviews all the related literature and research paper to apply with this project. Understand the cause of the Ischemia reperfusion injury, mechanisms of how Rapamycin and Colchicine treat Ischemia reperfusion injury, double emulsion nanoparticles technique and the advantages of this technique.

Chapter 3 describes the equipment and materials required. Steps for the double emulsion nanoparticles experiment start with the practicing of single emulsion of Rapamycin.

Chapter 4 provides the result obtained from the percent encapsulation efficiency and percent drug loading in the form of tables, graphs, and images. Additionally, the outcomes of the characterization method of Dynamic light scattering (DLS) to determine the sized of nanoparticles and Zetapotential to observe the surface of nanoparticles synthesized.

Chapter 5 summarizes the major findings of this study and provide recommendations for further study plan.

CHAPTER 2
REVIEW OF THEORY RELATED

This chapter discusses the theory regarding the knowledge applied during the experiment according to the objective stated above. Including the knowledge about the cause and the mechanisms of the ischemia-reperfusion injury, the principles of the double emulsion nanoparticle, the history, properties and mechanisms of Rapamycin and Colchicine which are the drugs that have been used for encapsulation as double emulsion nanoparticles, the devices utilized for creating the nanoparticles, and to observe encapsulation and drug loading efficiency.

2.1 Introduction of Ischemia Reperfusion injury

Restoring blood flow is crucial in cases where an organ or a particular tissue area isn't receiving enough blood to prevent irreversible tissue necrosis and maintain organ function. Reintroducing oxygenation and perfusion following ischemia, however, may cause a counterintuitive reaction that prevents the organ's initial blood supply. The abnormal condition known as ischemia-reperfusion (IR) injury exacerbates pathologies in various emergency medicine scenarios, such as hemorrhagic shock resuscitation, acute coronary syndrome, limb injuries, and cerebral ischemia [7].

2.1.1 Mechanism of IR injury

Mechanisms of IR injury can be generally divided into two states of ischemic state and reperfusion state.

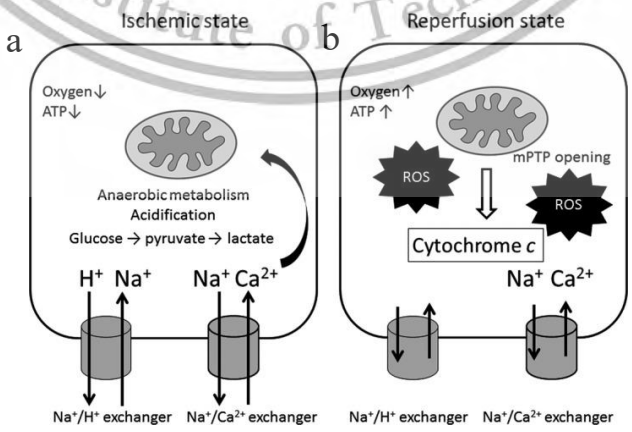

Figure 1. Diagram illustrating the sequential changes in cytosolic and mitochondrial functions during the process of ischemic state(a) reperfusion state(b).

Figure 1 shows the condition of oxygen deprivation (hypoxia), a reduction in oxygen levels induces anaerobic glycolysis, resulting in an accumulation of H^+ in cytosolic lactate, leading to acidification. This acidification triggers the activation of the Na^+ H^+ exchanger, causing an increase in cytosolic Na^{2+}, which, in turn, activates the Na^+ Ca^{2+} exchanger, causing elevated levels of cytosolic Ca^{2+}. The overload of cytosolic Ca^{2+} subsequently impacts the Ca^{2+} levels in the mitochondrial matrix. This overload disrupts the process of transporting electrons, resulting in an increase of the level of reactive oxygen species (ROS). The compromised respiration and substrate utilization contribute to a reduction in the production of adenosine triphosphate of the mitochondria.

For the reperfusion stage (Figure 1 a), heightened mitochondrial permeability transition pore (mPTP) activity amplifies the generation of reactive oxygen species (ROS) and disturbs the intracellular distribution of Ca^{2+}, Na^+, and pH, leading to eventual irreversible cell death. As the levels of ROS continue to increase, mitochondria endure more profound damage, prompting the opening of mPTP and the release of cytochrome C, consequently initiating apoptosis.

2.1.1.1 Ischemic state

The fundamental mechanism of mitochondria is to generate ATP through oxidative phosphorylation. Inhibition of oxidative phosphorylation, as observed in ischemic conditions, disrupts normal cellular processes.

Within the mitochondria, ischemia induces anaerobic metabolism and dysfunction in the electron transport chain, resulting in reduced ATP production. The decline in ATP production causes malfunction of Na^+-K^+-ATPase, leading to elevated levels of intracellular calcium, hydrogen, and sodium. This, in turn, causes cell swelling and impairs cytoplasmic enzyme activity. Excessive calcium levels can cause cellular damage through various mechanisms, including the destruction of cell membranes, initiation of cell death, and disruption of mitochondrial function [8]. Another relevant mechanism in the pathophysiology of ischemia-induced injuries involves the limitation of prolyl hydroxylase enzymes that sense oxygen. Since these enzymes require oxygen as a co-factor, inhibiting prolyl hydroxylase enzymes due to oxygen deprivation promotes the activation of hypoxia-inducible factor

(HIF) and inflammatory signaling pathways. This inhibition helps stimulate the response to oxygen deprivation and signaling cascades post-transcriptionally. Controlling the stability of decoding factors in the subsequent period, such as nuclear factor-kappa B (NF-κB) and factors contributing to hypoxia, consequently, leads to alterations in gene expression during ischemia.

2.1.1.2 Reperfusion state

During the reperfusion phase (figure 1 b), extensive damage to mitochondria and disruptions in electrolyte balance result in the rapid generation of significant amounts of reactive oxygen species (ROS) within minutes. These ROS originates from diverse sources, including heightened enzymatic activity of xanthine oxidase, nicotinamide adenine dinucleotide phosphate oxidase (NOX), cyclooxygenase, lipoxygenase, and inducible nitric oxide synthase (iNOS). Additionally, reactions within the mitochondrial electron transport chain and the oxidation of catecholamines contribute to this phenomenon [9]. Reactive oxygen species, consisting of molecules or fragments with unpaired electrons like peroxynitrite, superoxide, hydrogen peroxide, and hydroxyl radical, are responsible for inducing damage to cell and organelle membranes, causing single-strand DNA breakage, enzyme inactivation, and activating the nuclear enzyme poly (ADP-ribose) synthetase. Consequently, these processes lead to various forms of cell death, including necrosis, apoptosis, autophagy, mitoptosis, and necroptosis. Furthermore, a cascade known as lipid peroxidation, resulting in the oxidation of polyunsaturated fatty acids, disrupts the structure of biological membranes and produces detrimental byproducts such as malondialdehyde [10].

Ischemia-reperfusion injury initiates a sophisticated set of inflammatory immune responses in the absence of pathogenic triggers, a phenomenon known as sterile inflammation. Sterile inflammation encompasses a sequence of signaling events facilitated by pattern-recognition receptors like Toll-like receptors (TLRs), involving the recruitment and activation of cells from both the adaptive and innate immune systems, as well as the activation of the complement system [11]. Toll-like receptor, a crucial pattern-recognition

receptor, assumes a significant role in orchestrating the inflammatory response during organ injury in the context of ischemia-reperfusion.

Upon entering the post-reperfusion phase, danger-associated molecular patterns, which include substances such as peroxiredoxin, high mobility group box-1, nucleotides, purines, and nucleic acid fragments, are released, initiating an inflammatory response. These patterns bind to innate immune receptors like TLRs and purinergic receptors on microglia and leukocytes, activating them and subsequently triggering inflammatory transcription factors such as NF-κB, activator protein 1, and mitogen-activated protein kinase [12]. This activation leads to the production of cytokines, chemokines, adhesion molecules (such as intercellular adhesion molecule-1 or E-selectin), matrix metalloproteinase-9, iNOS, and NOX, intensifying the damage caused by ischemia. Moreover, the cellular process of autophagy, responsible for degrading damaged or unnecessary proteins and organelles, also contributes to the injury induced by ischemia-reperfusion [13]. Despite the generally protective role of an acidic pH during ischemia, it is rapidly normalized following reperfusion, paradoxically believed to enhance cytotoxicity.

2.2 PLGA Double-emulsion nanoparticles

2.2.1 Nanoparticles

Poly (lactic-co-glycolic acid) (PLGA)belongs in the functional group of aliphatic polyester family and is a biodegradable polymer well-recognized for its biocompatibility. It has gained popularity in drug delivery applications, given its FDA approval for use in humans as resorbable sutures. PLGA serves as a carrier for both hydrophobic and hydrophilic medications, encapsulating them in the form of particles through the process of creating an emulsion. To elaborate, the medication is either dissolved within the polymer or emulsified with the polymer in an organic phase before being emulsified with an aqueous phase. After solvent evaporation, particles are collected through centrifugation and prepared for extended storage via lyophilization. PLGA gradually degrades in aqueous environments through hydrolysis, enabling the gradual release of encapsulated chemicals over weeks to months. Despite PLGA's numerous advantages in drug administration, the consistent production of nanoparticles poses challenges. Variability can be introduced by employing different equipment,

variations in reagent batches, and specific emulsification processes. For the characterization of the nanoparticles synthesized of either single or double emulsion techniques, using scanning electron microscopy (SEM) to determine the particle size [14].

In recent decades, polymers have gained popularity as effective carriers for drug delivery across various applications, from targeted tumor therapy to regulating the immune system. When medications are either encapsulated or chemically linked to polymers, their performance often surpasses that of freely administered drugs. This is attributed to the protective role of the polymer, preventing drug degradation, resulting in an extended biological half-life and the potential for increased efficacy while minimizing systemic side effects. Among the various polymers, PLGA stands out as an exemplary nanoscale delivery method due to its capacity to provide sustained release of encapsulated medications and subsequent degradation into biocompatible byproducts like lactic and glycolic acid. PLGA has proven ideal for delivering small compounds, proteins, and nucleic acids, demonstrating enhanced therapeutic activity across various disease applications. Notably, this material platform offers flexibility in terms of particle size, charge, and the presentation of ligands on the particle's surface, facilitating targeted distribution to specific tissues or imaging. Additionally, PLGA's existing use in humans as biodegradable sutures (e.g., Purasorb, Purac Biomaterials, and Vicryl, Ethicon Inc.) adds to its promise for potential clinical applications [15].

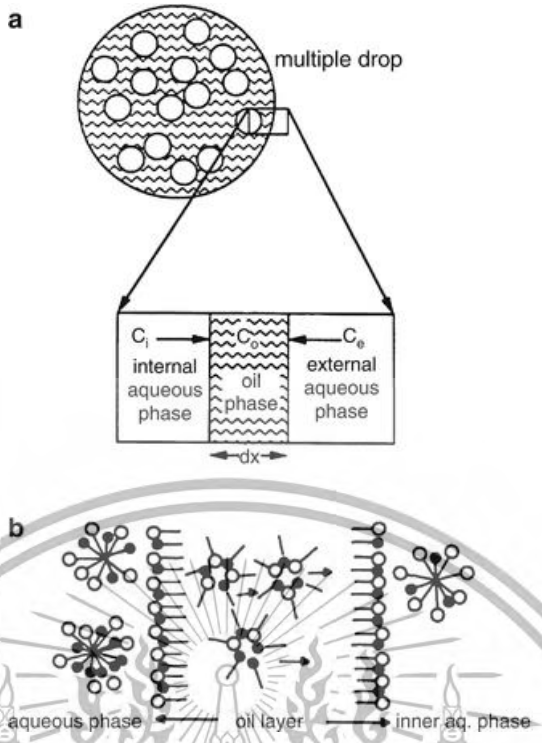

*Figure 2. Schematic illustration of the two possible transport mechanisms. (**a**) Lamellar thinning and (**b**) reverse micellar transport of marker from the inner aqueous phase to the continuous aqueous phase*

Figure 2 shows the method of using PLGA to encapsulate hydrophilic and hydrophobic medicines at micro- or nanoscale dimensions is to create an oil-water single emulsion or a water-oil-water double emulsion. To clarify it simply, PLGA is emulsified with water after being dissolved in an organic phase (oil). Hydrophilic drugs, which are soluble in water, can be first emulsified with the polymer solution prior to particle formation, whereas hydrophobic drugs are integrated directly into the oil phase. Using bursts of high-intensity sonication makes it easier to form smaller polymer droplets. In order to allow the solvent to evaporate, the resulting emulsion is subsequently added to a larger aqueous phase and stirred for several hours. The resulting stiffened nanoparticles are then collected and centrifuged to wash them [3].

2.3 Rapamycin

Rapamycin is widely known and was initially discovered on Easter Island, isolated from a Gram-positive aerobic soil bacterium called Streptomyces hydroscopicus AY B-994 (NRRL 5491). It derived its name from the indigenous title of the island, Rapa Nui. Research conducted in the 1970s and 1980s unveiled its dual functionality as a potent inhibitor of fungal cell growth and an immunosuppressive and anticancer medication for humans. The observation that rapamycin affects both yeast and human cells immediately suggested a shared mechanism of action, leading to groundbreaking research in the 1990s that identified the highly conserved TOR kinase, also known as mTOR. After the discovery of TOR, the field experienced a surge of studies exploring how this kinase and its associated partners constitute a central component of a complex signaling network governing nearly all aspects of growth and metabolism. In fact, the dysregulation of TOR is implicated in various human diseases, including cancer, and plays crucial roles in aging, as well as responses to environmental and nutritional stress [16].

The less widely acknowledged pathway involves the S. hydroscopicus strain separated from Easter Island, transported to the laboratory of pharmacology researchers at Ayerst Research Laboratories, later known as Wyeth-Ayerst and Wyeth. It was in this setting that Rapamycin was isolated and characterized. Furthermore, the clear reason for the initial journey to Easter Island by the international team of scientists and physicians was not widely understood. This part of the story has been pieced together to provide a relatively limited overview in METEI, in stark contrast to Stanley's Dream, which was published shortly before the onset of the COVID-19 pandemic. Stanley's Dream presented a comprehensive narrative resulting from fortunate access to extensive survey documents, including primary data from studies involving the islanders (Rapanui) and personal notes from the Meteti Expedition members. Duffin also sought and interviewed surviving island expedition members or, in many cases, their diligent descendants. In the end, she personally visited the island to meet the surviving Rapanui who had connections with the expedition members and participated in METEI's study [17].

Rapamycin is recognized as the primary small molecule inhibitor of mTOR. However, the broad spectrum of medical conditions linked to mTOR irregularities has paved the way for the development of novel drugs targeting this pathway. The first wave of mTOR inhibitors, referred to as first-generation mTOR inhibitors or rapalogs, is specifically designed to directly impede the mTOR complex. Their mechanism involves inhibiting the binding of raptor, consequently impeding mTOR activation and its capacity to phosphorylate downstream molecules. Medications such as sirolimus and temsirolimus belong to these first-generation inhibitors [18].

More advanced and sophisticated second-generation mTOR inhibitors not only reduce cell cycle progression but also inhibit protein synthesis. These specific compounds have the capability to direct their impact either towards the AKT or the S6K pathways. Theoretically, this selectivity can influence either cell death and the initiation of autophagy (mTORC1) or cell survival and functionality (mTORC2). However, given that the initial generation of inhibitors has been the primary choice in the majority of preclinical investigations and notably possesses extensive clinical safety records, this review will focus on the utilization of these substances specifically in the context of cerebral ischemia [19].

2.3.1 Rapamycin properties

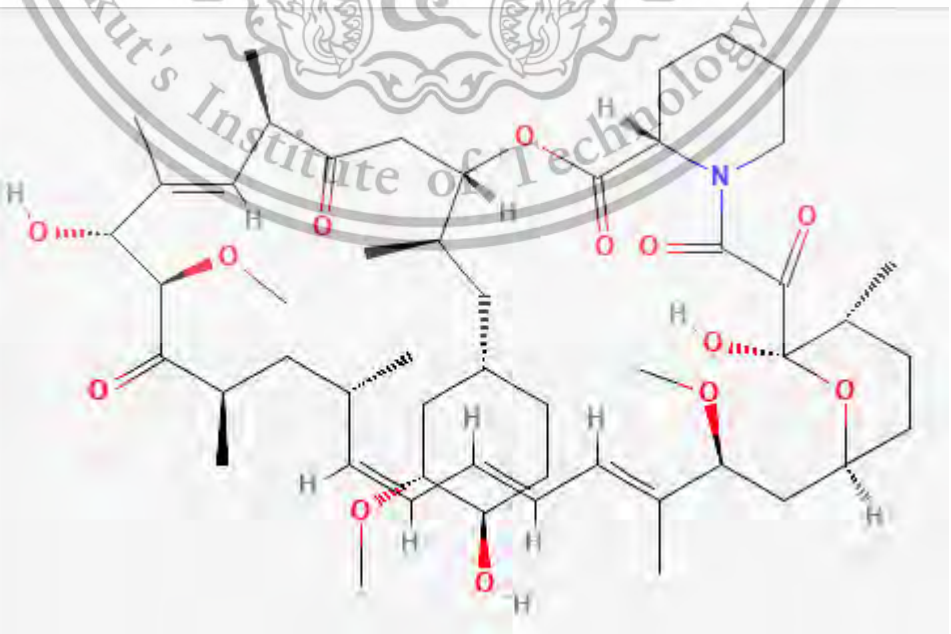

Figure 3. Chemical structure of Rapamycin

The chemical structure of Rapamycin contains a complex arrangement of carbon, hydrogen, oxygen, and nitrogen atoms. It is a large, macrocyclic molecule with a molecular formula of is $C_{51}H_{79}NO_{13,}$ as shown in the figure 3. The structure includes multiple rings and functional groups, which contribute to its biological activity as an mTOR inhibitor with the molecular weight of 914.17 and soluble in DMSO at 50mg/ml or methanol at 25mg/ml, soluble in alcohol, dimethyl sulfoxide and dimethyl formamide. Insoluble in water [20].

2.3.2 Molecular mechanism of Rapamycin

The mTOR pathway serves as a central hub for integrating signals from diverse stimuli. Recent studies indicate that mTOR activation occurs in response to stimulation by Toll-like receptors (TLRs). While there is a more comprehensive understanding of the regulatory mechanisms both upstream and downstream of mTORC1, mTORC2 remains less explored. The mTORC1 pathway is stimulated under conditions such as acidic deprivation, oxygen deprivation, energy stress, endoplasmic reticulum (ER) stress, genetic stress-induced protein kinase AMP-activated protein kinase (AMPK), a crucial cellular energy sensor. In response to growth signals, mTORC1 promotes phosphorylation and activates ribosomal protein S6 kinase 1 (S6K1), which enhances mRNA production efficiency and initiates protein translation. Conversely, mTORC1 inhibits the initiation factor 4E-binding protein 1 (4E-BP1), leading to the formation of the eIF4F complex, initiating cap-dependent translation. Moreover, mTORC1 promotes glucose metabolism by decoding the toxic response to hypoxia-inducible factor-1α (HIF-1α), controlling mitochondrial function, and catabolism through peroxisome-proliferator-activated receptor coactivator-1α (PGC-1α) pathway, promoting fatty acid synthesis. In turn, mTORC1 inhibits the initiation of uncapped translation factor 4E-binding protein 1 (4E-BP1), resulting in the initiation of eIF4F complex-dependent translation. Furthermore, mTORC1 enhances glucose metabolism through the decoding of toxic responses to hypoxia-inducible factor-1α (HIF-1α), controlling mitochondrial function, and catabolism through the peroxisome-proliferator-activated receptor coactivator-1α (PGC-1α) pathway, promoting fatty acid synthesis. In the reciprocal pathway, mTORC2 is triggered by the PI3K pathway stimulated by growth factors and impacted by reduced nutrient availability [21]. The specific mechanism behind this stimulation is not fully understood, except that it involves the relationship between mTORC2 and ribosomes. Recent discoveries

indicate the critical role of ribosomes in mTORC2 activity, suggesting a link between cell growth potential and mTORC2. Additionally, mTORC1 appears to inhibit mTORC2 through Rictor phosphorylation, indicating collaboration between mTORC1 and mTORC2. The target of rapamycin complex 2 (mTORC2) in mammals acts as a kinase that triggers the initiation of AGC (protein kinase A, protein kinase G, protein kinase C) family members, including Akt, a crucial oncoprotein that stimulates a broad anti-apoptotic program, promoting cell survival. Moreover, mTORC2 influences components of the protein kinase C (PKC) family and Ras homolog A through the regulation of cardiolipin/cytosolic disorders, emphasizing its recent role in cell motility, invasion, and metastasis [22].

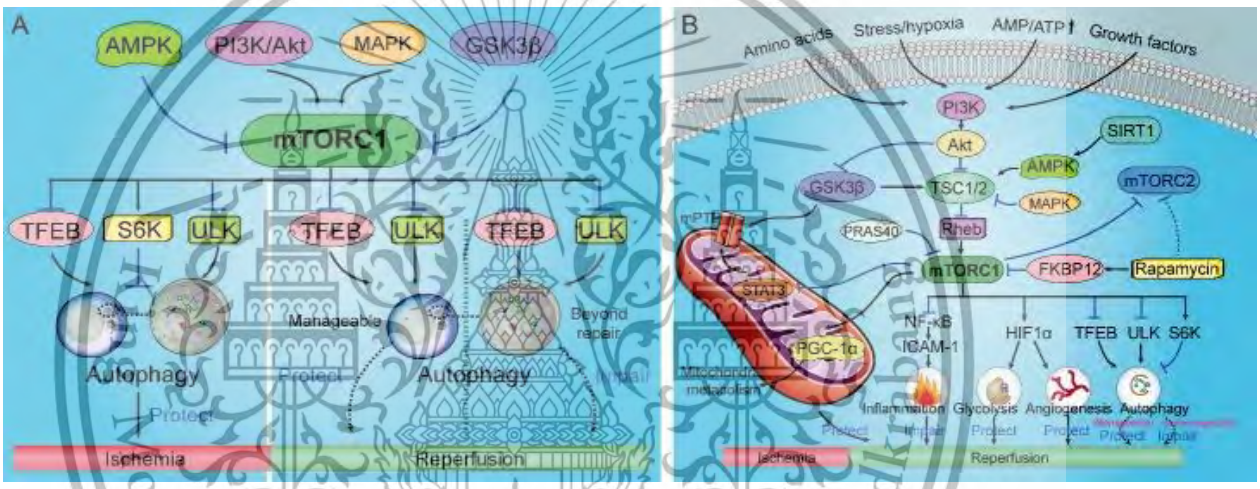

Figure 4. Mechanism of mTOR to inhibit autophagy

2.3.3 mTOR related autophagy of Ischemic reperfusion injury

The mTOR plays a crucial role as a key regulator in autophagy inhibition, contributing to the facilitation of the autophagic process (Figure 4). Autophagy, commonly known as "self-eating," is a lysosomal degradation pathway responsible for the elimination of aggregated proteins and damaged cellular components. This process is vital for maintaining cellular homeostasis under various physiological and pathological conditions. Studies suggest that autophagic degradation tends to decrease with age, potentially leading to the accumulation of cellular damage, such as protein aggregates and dysfunctional mitochondria. The mTORC1 serves as a central controller of autophagy, influenced by various factors like energy depletion and blood deficiency. The activation of mTORC1 stimulates p70S6K1 significantly while concurrently inhibiting the transcription factor EB (TFEB), a key regulator of autophagy. This

inhibition results in the suppression of autophagy-related proteins, including Atg7, crucial for autophagic protein turnover. Notably, mTORC1 phosphorylates ULK1/2, associated with the autophagic unc-51-like 1/2 (ULK1/2) complex, thereby inhibiting ULK1/Atg13/FIP200 macrocomplex formation responsible for promoting autophagosome formation. Furthermore, mTORC1 activation suppresses the expression of autophagic proteins, with particular importance given to Atg7, a critical initiator of autophagy as shown in figure 4. Aberrations in the control of autophagy are implicated in various age-related diseases, including diabetes, cardiovascular disorders, and neurodegenerative conditions. It is proposed that the improved autophagic flux resulting from mTORC1 inhibition in these disease models contributes to the observed benefits. In times of energy and blood deficiency, mTORC1 is inhibited, conserving cellular energy and promoting autophagy, ultimately supporting cell survival [23].

It has been observed that activating autophagy through AMPK, which inhibits mTOR, can help alleviate injuries from ischemia and enhance the viability of stem cells from tissues [24]. However, the roles of mTOR signaling and autophagy in restoring injuries to their original state remain debated. Inhibiting autophagy using the prominent negative regulator Atg5 helps reduce the size of ischemic preconditioning (IPC)-induced dead heart muscle cells in HL-1 cells, suggesting a protective role for autophagy in ischemic heart muscle injury and recovery. Ischemic postconditioning (IPostC) increase the expression of proteins related to autophagy and using the autophagy inhibitor 3-methyl-adenine pharmacologically reduces the size of IPostC-induced dead heart muscle, indicating the potential pharmacological impact of autophagy inhibition in recovery [25]. However, other studies suggest that pharmacologically induced autophagy may have detrimental effects during recovery. Inhibition of autophagy through pharmacological modulation with urocortin, an extracellular heart peptide, helps reduce cell death in recovering heart muscle after ischemia. Additionally, a combination of four active compound types reduces injuries from ischemia-reperfusion by modulating autophagy and the AMPK/mTOR and JNK pathways. Autophagy acts as an adaptive response to maintain cell survival under stressful conditions. If cellular stress becomes excessive and leads to irreversible damage, stimulating autophagy may push cells towards programmed cell death [26]. This suggests that pharmacologically induced autophagy may either protect or cause damage from injuries due to ischemia upon recovery in tissues or organs, depending on

the level of autophagic stimulation and specific experimental contexts. Thus, maintaining controlled levels of autophagy through mTOR signaling may be a valuable strategy for treating ischemia-induced injuries. The decision to treat injuries with ischemia-induced autophagy may depend on the level of autophagic stimulation and the specific experimental context. Therefore, appropriately controlling autophagy levels through mTOR signaling may be a valuable strategy for treating ischemia-induced injuries [27].

2.4 Colchicine

Colchicine is an alkaloid with a preference for lipophilic compounds, characterized by a tricyclic structure. It is derived from plants such as Colchicum autumnale (autumn crocus) and Gloriosa superba (glory lily), found in various plant parts, including seeds and flowers. Its medicinal use dates back to ancient times, with records from over 3,000 years ago in the ancient Egyptian medical document known as the Ebers Papyrus. The ancient Greek physician, Theophrastus of Eresus, in his work "Therapeutica" (circa 550 BCE), recommended the use of colchicum [28], also known as "hermodactyl" or "the finger of Hermes," for treating gout. Colchicine has maintained its reputation over many centuries. However, it has been widely recognized that colchicine should be used cautiously and that its repeated or excessive use may be ineffective or harmful.

A significant change occurred in the late 17th to early 18th centuries when colchicine was once again utilized for treating gout in Europe. In 1819, Pelletier and Caventou identified a substance from the root of Colchicum autumnale, and in 1833, Geiger refined this substance, naming it colchicine [29]. The pharmacist Alfred Houdé later enhanced the production process in 1887, resulting in the manufacture of purified colchicine.

Colchicine has been shown to inhibit a number of inflammatory pathways, with gout being the main clinical indication for its use. Monosodium urate crystals build up in the joints, causing a strong inflammatory response that leads to the influx of immune cells including dendritic cells, neutrophils, and macrophages/monocytes, which causes extensive tissue damage. Colchicine has a significant impact on active neutrophils, a major source of immune cells in joint fluid and an essential component in crystal-induced inflammation, even if it has no direct effect on urate crystal accumulation [30].

The production of several inflammatory chemicals by these activated immune cells, such as TNFα, IL-1β, IL-6, and IL-8, leads to an increase in the expression of adhesion molecules such as VCAM-1 and E-selectin on the surface of endothelial cells. Additionally, urate crystals promote neutrophils' generation of superoxide anions, which is necessary for the NLRP3 inflammasome complex—known to be involved in gout attacks—to be activated. As previously mentioned, colchicine builds up in immune cells and inhibits the release of cytokines, which reduces the inflammatory response. Furthermore, it reduces the recruitment of neutrophils via adjusting the expression of E-selectin on the surface of endothelial cells. Colchicine reduces TNF production in macrophages and TNF-receptor expression in both macrophages and endothelial cells by impairing vesicular trafficking [31]. However, it's important to note that disrupting the microtubular network could adversely affect various essential cellular processes. Colchicine also carries a risk of multi-organ toxicity in case of overdose and is associated with several known adverse reactions. Common side effects include gastrointestinal symptoms like diarrhea, vomiting, and nausea, while less frequent symptoms involve myopathy, hematologic disturbances, and muscle weakness. Furthermore, colchicine may directly impact cardiomyocytes, interfering with their contractile and conduction properties [32].

Colchicine, a microtubule polymerization inhibitor, has been demonstrated to mitigate ischemia-reperfusion (IR) injury in various tissues by employing multiple mechanisms: it inhibits neutrophil function, decreases the release of inflammatory cytokines, hinders leukotriene production, and modulates TNF-α activity. Colchicine significantly reduced lipid peroxidation and lowered levels of inflammatory cytokines in IR-injured muscle tissues. However, further research is needed to establish dose-effect relationships, assess clinical efficacy, and investigate colchicine's impact on remote organ dysfunction following IR injury [33].

2.4.1 Colchicine properties

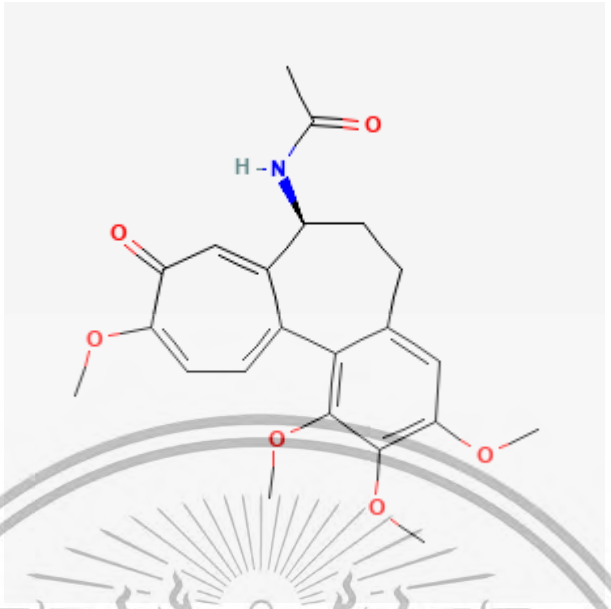

Figure 5. Chemical structure of colchicine

Figure 5 shows, The Colchicine that has a chemical formula of C22H25NO6 and a full chemical name of N-[(7S)-5,6,7,9-tetrahydro-1,2,3,10-tetramethoxy-9-oxobenzo(a)heptalen-7-il)acetamide]. This compound consists of three distinct rings: Ring A, characterized by a tricyclic phenyl structure; B-ring, with seven members; and the C-ring, featuring a methoxytropone structure [20]. The A and C rings maintain structural stability by interacting with tubulin, playing a crucial role in their relationship. Colchicoside, an analog of colchicine with a major modification in the A-ring, loses the ability to form complexes with tubulin. Similarly, alterations in the structure of the C-ring, as observed in isocolchicine, result in compounds that lack efficacy and tubulin binding [34].

2.4.2 Colchicine mechanism of action

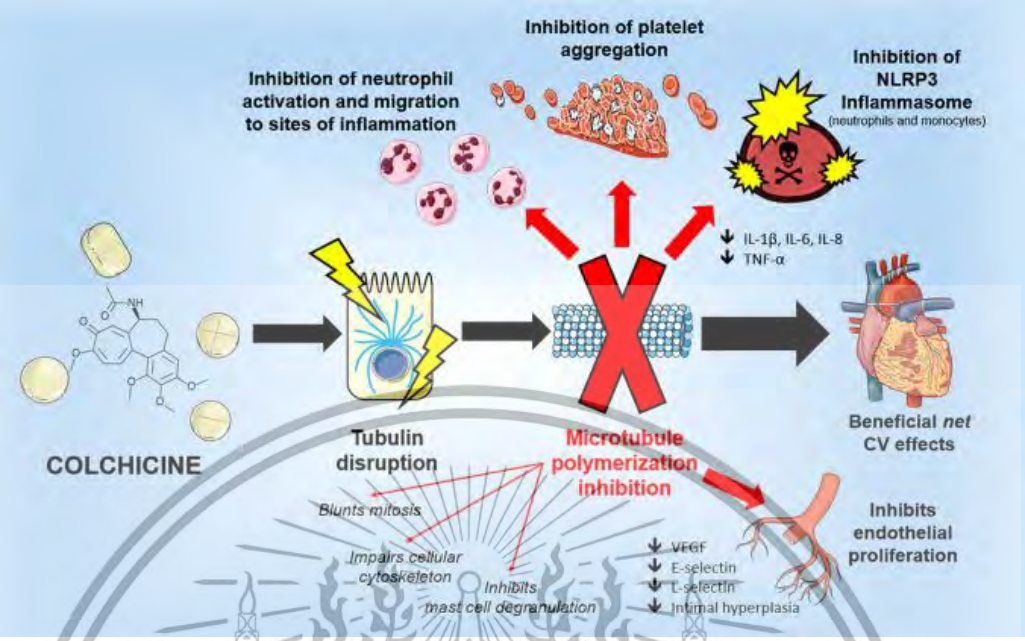

Figure 6. Mechanism of Colchicine – colchicine primarily causes tubulin disruption and prevents microtubule formation, hence resulting in neutrophils inhibition, anti-inflammatory effects, beneficial cardiovascular effects and inhibiting endothelial cells proliferation.

Figure 6 shows that early studies identified the microtubule as colchicine's principal target cellular structure. Temperature, pH, and tubulin concentration all affect how colchicine and tubulin interact with one another [35]. This interaction involves a 1:1 molar ratio of colchicine to tubulin dimer, resulting in a non-covalent binding that is difficult to reverse [36]. According to the widely accepted concept, this reversible binding is followed by gradual conformational changes that make the original complex more stable and difficult to reversible. When tubulin heterodimers are bound by colchicine, their spatial arrangement is disrupted, which results in tubulin disruption and prevents further microtubule formation. Essential cellular functions such as cell division, migration, organelle transport, and cytokine/chemokine secretion depend on microtubule dynamics [37].

2.5 Nanodrop One C Microvolume UV-Vis Spectrophotometer

Figure 7. NanoDrop OneC Microvolume UV-Vis Spectrophotometer

Nanodrop One Microvolume UV-Vis Spectrophotometers quantify and qualify DNA, RNA, and protein samples in seconds with use of 4-5 µL and obtain full-spectral data. With spectral range from 190-280nm for measuring a variety of samples type such as peptides, DNA and RNA, Purified protein, Toxicology assays and industrial dyes, gold nanoparticles, Colorimetric protein assays and Optical density measurements as shown in the figure 7.

2.6 Standard Curve

In analytical chemistry the standard curve is a method for determining the concentration of an unknown sample by comparing the unknown to the standard sample of known concentration. In more general use, a calibration curve is a graph or a table that is used with measuring devices to infer values for the desired quantity from the sensor output by indirectly evaluating certain characteristics. For example, to calculate the applied pressure from the transducer's output, which is usually voltage, a calibration curve may be created for that specific pressure transducer. When an instrument uses a sensor whose calibration fluctuates between samples, changes over time, or changes with usage, this kind of curve is frequently used. The instrument can be directly calibrated using the measured unit when the sensor output remains stable.

The operator creates different reference samples with various concentrations, aiming to get close to what's in the unknown sample. These concentrations should work with their equipment. After analyzing these reference samples using their equipment, they collect a set of numbers. Usually, when they plot how the equipment reacts to these

numbers against the concentration, it forms a straight line. Then, when they test the unknown sample, they can use this line to estimate how much of the substance is in it.

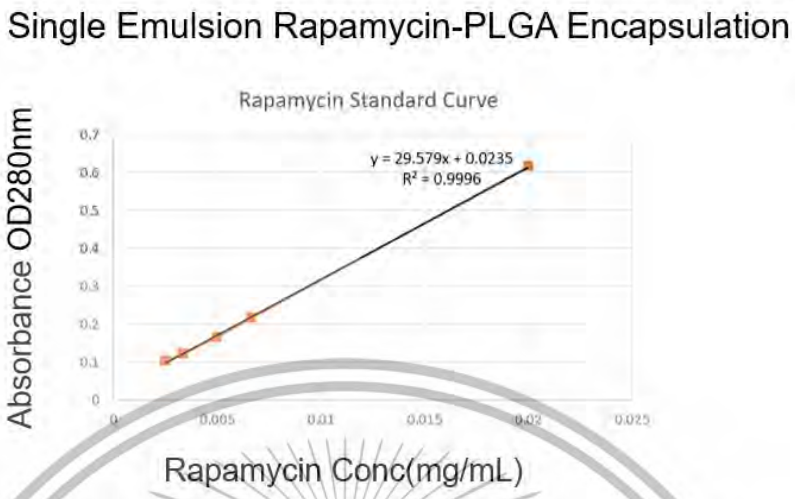

Figure 8. Standard Curve of Rapamycin single emulsion

Figure 8 state the information, which includes both the analyte concentrations and the instrument's responses for each standard, can be used to create a straight line through linear regression analysis. This results in a model expressed as the equation y = mx + C, where y represents the instrument response, m stands for the sensitivity, and C represents a constant that characterizes the background. With this equation, the concentration of the analyte (x) in unknown samples can be determined.

2.7 Probe sonicator

Figure 9. Probe Sonicator

The intense shear forces generated through ultrasonic cavitation possess the capability to disintegrate particle agglomerates (figure 9), resulting in reduced particles sizes and greater uniformity. The stable and homogenous suspensions achieved through ultrasonic methods find broad applications across various industries

today. Probe sonication is particularly efficient in handling nanomaterials such as carbon nanotubes, graphene, inks, metal oxides, and more. Sonicators have emerged as the established industry standard for dispersing, Deagglomerating, Particle size reduction, Particle synthesis and precipitation and surface functionalization [38].

2.9 Dynamic Light Scattering (DLS)

Dynamic Light Scattering (DLS) is an optical method utilized for examining the dynamic characteristics and size distribution of a diverse range of physical, chemical, and biological systems containing multiple suspended components. These components may include colloidal particles, macromolecules, bubbles, or droplets, and for simplicity, we will refer to them collectively as particles. The principle behind DLS involves extracting spectral information from the time-dependent fluctuations in the light scattered from a spatially limited volume within the sample. Specifically, when a suspension of particles is exposed to a monochromatic coherent light beam, the resulting scattered light waves disperse in all directions. The interference of scattered waves in the far-field region generates a net scattered light intensity, denoted as Is(t). Due to the random motion of the suspended particles in the sample, the interference can stochastically be either constructive or destructive, leading to a stochastic light intensity signal. The colloidal particles in the investigated dispersion undergo Brownian motion, causing fluctuations in the distances between the particles and, consequently, fluctuations in the phase relationships of the scattered light. Moreover, the number of particles within the scattering volume may vary over time. The overall outcome is a fluctuating scattered intensity [39]. The corresponding measured normalized intensity correlation function is expressed as:

$$g_2(q,\tau) = \frac{\langle I_s(q,t) I_s(q,t+\tau) \rangle}{\langle |I_s(q,t)|^2 \rangle},$$

T for time lag and q is scattering vector module. By Siegert relation can be related to the electric field correlation function g1(q,T):

$$g_2(q,\tau) = 1 + \beta \, |g_1(q,\tau)|^2$$

B being the intercept and the field correlation function g1(q,T) is defined as

$$g_1(q,\tau) = \frac{\langle E_s(q,t))E_s^*(q,t+\tau)\rangle}{\langle |E_s(q,t,)|^2\rangle}$$

The field correlation function may be used to determine the diffusion coefficient D of the scatterers. A monodisperse sample is fitted to an exponential function.

$$g_1(q,\tau) = \exp(-\Gamma\tau)$$

Γ, the decay rate yield from:

$$\Gamma = q^2 D$$

Obtains the diffusion coefficient D by using the Stokes-Einstein equation one can calculate the hydrodynamic radius.

$$R = \frac{kT}{6\pi\eta D}$$

with k the Boltzmann constant, T the temperature in Kelvins, and η the viscosity of the suspending medium.

For reminder, the equation above is only true for the single scattered light case. If the concentration of the particle is too high, meaning that free path *l* becomes smaller than the sample dimension *d*, multiple scattering will occur which will render the equation invalid [40].

2.10 Zeta Potential (ZT)

Zeta potential, occasionally called electrokinetic potential, is an interfacial property commonly measured in millivolts. It occurs at the interface of any material upon contact with a liquid medium. An electrochemical double layer is formed when a substance comes into contact with a liquid. This is because the functional groups on the material's surface interact with the surrounding medium, creating a surface charge that attracts ions that are oppositely charged. The total of the initial surface charge and the accumulated layer is known as the zeta potential. When discussing zeta potential, there are a few important things to keep in mind. First, it exists when a material interacts with a liquid; in these situations, it represents the effective net charge. It can be studied with dispersed particles and macroscopic surfaces, such as membranes,

hair, and polymers. It can be measured on macroscopic surfaces (e.g., membranes, hair, polymers) as well as particles dispersed in a liquid (e.g., colloids, nanoparticles, liposomes), and distinguishing between them is critical for choosing the proper measurement technology. Furthermore, the properties of the liquid medium, particularly the pH and buffer content, have a substantial impact on the development of the zeta potential. Notably, solid solids (at the solid-liquid interface) and liquid droplets (at the liquid-liquid interface) can be observed on a surface charge [41].

Measuring the zeta potential provides insights into surface properties, particle stability, and how dissolved compounds interact with solid surfaces. Understanding the zeta potential of larger surfaces is essential for understanding how solid materials behave in various water-based technical processes, such as water treatment membranes, biomaterials in contact with blood, and semiconductor wafer wet processing. Understanding a material's zeta potential benefits, the optimization of surface alterations to ensure the material functions efficiently in its intended applications. When it comes to particles, the zeta potential, which represents the ability of particles to separate from each other via electrical forces, is a significant indicator of colloidal dispersion stability, particularly that of nanoparticles or liposomes. In general, zeta potential values above ±30 mV indicate stable dispersions. The amplitude of the zeta potential alone indicates sample stability, whereas its sign indicates whether positive or negative charges dominate the surface. Aggregation, settling, and clumping are more likely to occur below ± 30 mV [42].

When nanoparticles or colloidal particles are suspended, they have a surface charge. The interaction between the charged particle and the applied field causes the particles to move when an electric field is applied. The motion's direction and velocity are determined by particle charge, suspending medium, and electric field strength. The Doppler shift in the dispersed light is then used to calculate particle velocity. The particle velocity is proportional to the particle's electrical potential at the shear plane, which is zeta potential. As a result, the optical measurement of particle motion under an applied field can be utilized to calculate zeta potential [43].

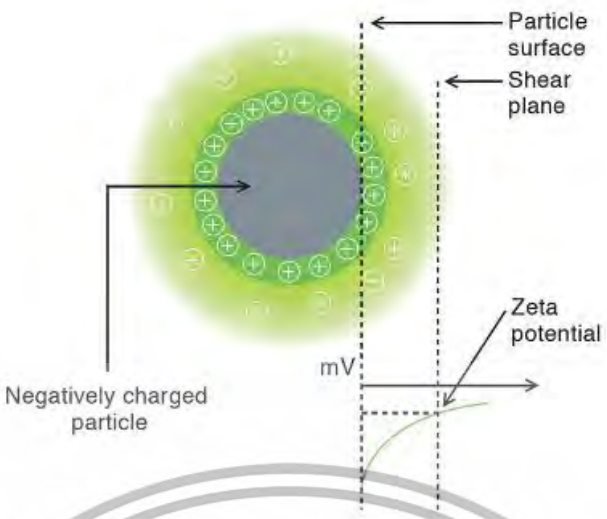

Figure 10. Particle motion under electric field

Figure 10 shows the Particle motion under an applied electric field known as electrophoresis. DelSa Nano C utilizes a technique known as laser Doppler electrophoresis. Particles of interest are suspended in a solution with a known refractive index (n), velocity (η), and dielectric constant (ε). The sample is irradiated by laser light of wavelength (λ). E is the strength of the electric field. The particles are moving as a result of the electric field. Because the particles are moving, the scattered light at the θ is measured, and the particle velocity V is determined using the frequency shift. The ratio of velocity to electric field strength V/E is then obtained. The mobility of zeta potential is then determined using a Smulochowski model [41].

$$U = \frac{\lambda \cdot V d}{2 \cdot E \cdot n \cdot \sin(\theta/2)}$$

This equation is used for the relationship between the calculated electrical mobility and zeta potential.

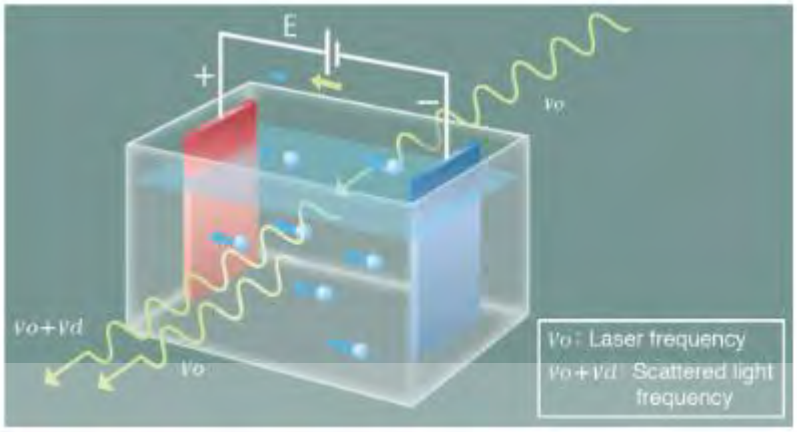

Figure 11. Zeta potential mechanics

$$\zeta = \frac{U\eta}{\varepsilon f(ka)},$$

where ζ – Zeta potential, U – Electrical mobility, E – Electric field strength, ε – Solvent dielectric constant, n – Solvent refraction index, η – Solvent viscosity, f(ka) – henry coefficient as shown in the figure 11.

CHAPTER 3
METHODOLOGY

Methodology describes in detail the preparation of solutions, equipment, and methods used in this experiment. The project overview begins with the preparation of materials including from PVA for the outermost layer of the nanoparticles and the two main drugs, Rapamycin and Colchicine. Followed by an overview of the required equipment and materials. In the following section, we provide the experimental protocols and explanations for each step, along with recommendations if the experiment needs to be repeated.

3.1 Material used to prepare before starting the experiment

3.1.1 PVA preparation

Nanoparticles encapsulated into layers of aqueous layer and oil layer, need to be encapsulated with the aqueous layer of PVA for the most outer layer of the nanoparticles. This step needs to prepare the PVA from the substance in the form pf particle to the solution of the PVA with 1% concentration. After that PVA prepared need to sterile with sterilizer as for using to synthesize the drug then stored in the 4C temperature environment for further use.

3.1.2 Rapamycin, Colchicine and PLGA preparation

For the preparation of colchicine, could be administered at room temperature. Conversely, for PLGA and Rapamycin, it is recommended to prepare an ice bath to maintain their optimal condition throughout the experiment.

3.2 Equipment and Material

This section is about the materials and equipment that are being used to conduct the experiment.

3.2.1 Lab Equipment

1. Micropipettes
2. Micropipettes
3. Pipette gun
4. Beaker

5. Autoclave Machine
6. Probe Sonicator
7. Nanodrop oneC

3.2.2 Materials

1. Rapamycin
2. Colchicine
3. Poly Lactic-co-Glycolic Acid (PLGA)
4. Dichloromethane (DCM)
5. Polyvinyl alcohol (PVA) 1%
6. Ethyl Acetate (EtAC)
7. Poly Vinyl Alcohol (PVA)
8. Phosphate Buffered Saline 1x (PBS 1x)
9. Ethanol (EtOH)

3.3 Experiment Protocol

3.3.1 Single Emulsion Nanoparticle

1. 100mg PLGA + 2.5ml DCM(O2), add 18.3 Rapamycin + 1ml EtOH(W2) into(O2).
2. Probe sonicator W1/O1/W2/O2: 2 minutes, 60% amplitude, with 30s pulses and 20s rests.
3. Add 10 ml 1% PVA(W3).
4. Probe sonicator W1-W3: 2 minutes, 60% amplitude, with 30s pulses and 20s rests.
5. Remove DCM: room temp for 15minutes 400rpm under vacuum pump.
6. Remove the remaining free Rapamycin and PVA by Ultra-centrifuged: 12k rpm for 10 minutes at $4^{O}C$ and wash with MQ water twice times.
7. The prepared NPs were protected and stored in 5ml MQ water at $4^{O}C$.

3.3.2 Double Emulsion Nanoparticle (Condition 1)

1. 30mg PLGA + 2.5 mL EtAc (O1), add 30mg Colchicine (W1)

2. Probe sonicator W1/O1: 2 minutes, 60% amplitude, with 30s pulses and 20s rests

3. 100mg PLGA + 2.5 mL DCM (O2), add 18.3mg Rapamycin+1mL EtOH (W2) into (O2)

4. Probe sonicator W1/O1/W2/O2: 2 minutes, 60% amplitude, with 30s pulses and 20s rests

5. Add 10 mL 1% PVA (W3)

6. Probe sonicator W1-W3: 2 minutes, 60% amplitude, with 30s pulses and 20s rests.

7. Remove DCM: Room temp. for 15 minutes 400rpm under a vacuum pump

8. Remove the remaining free Rapamycin, Colchicine and PVA by Ultra-centrifuged: 12k rpm for 15 minutes at 4^0C (once) and wash with MQ water twice times.

9. The prepared NPs were protected and stored in 5mL MQ water at 4^0C.

3.3.3 Double Emulsion Nanoparticle (Condition 2)

1. 30mg PLGA + 2.5 mL EtAc (O1), add 10mg Colchicine (W1)
   (Overnight PLGA + EtAc in 4^0C)

2. Probe sonicator W1/O1: 2 minutes, 60% amplitude, with 30s pulses and 20s rests

3. 100mg PLGA + 2.5 mL DCM (O2), add 18.3mg Rapamycin+1mL EtOH (W2) into (O2)

4. Probe sonicator W1/O1/W2/O2: 2 minutes, 60% amplitude, with 30s pulses and 20s rests

5. Add 10 mL 1% PVA (W3)

6. Probe sonicator W1-W3: 2 minutes, 60% amplitude, with 30s pulses and 20s rests.

7. Remove DCM: Room temp. for 15 minutes 400rpm under a vacuum pump

8. Remove the remaining free Rapamycin, Colchicine and PVA by Ultra-centrifuged: 12k rpm for 15 minutes at 4^0C (once) and wash with MQ water twice times.

9. The prepared NPs were protected and stored in 5mL MQ water at 4^0C.

3.4 Basic setup for probe sonicator to create nanoparticles

Figure 12. Setup for probe sonicator and seetting for Timer, Pulse and amplitude

The probe sonicator device Sonics Vibra Cell Ultrasonic Processor VCX 134 atft 130w 40khz (Figure 12) consist of three main parts, including the generator that provides electronic pulses, Converter that transform pulses into mechanical vibrations and the probe that transmit the vibration depend on the setting amplitude, duration of pules and rests and the timer for the purpose of size reduction, emulsification, dispersion nanoparticles.

3.5 Remove DCM using vacuum pump

Figure 13. Setup for removing DCM from the sample

The step of removing DCM administer in the fume hood by pouring the product into bottle neck with stir bar under 400rpm on the hot plate at the room temperature. Using liquid nitrogen (N_2) as a cold trap to eliminate any passing vapor of DCM is the most efficient way of removing DCM from your product in the vacuum pump as shown in Figure 13.

3.6 Centrifuge Machine

Figure 14. Centrifuge Machine using to separate the product

After the synthesized, we got the solution of nanoparticle and free Rapamycin, Colchicine and PVA that doesn't get encapsulated. Remove by using Micro Refrigerated Centrifuge Kubota Model 3700 (Figure 14) work based on the influence of gravitational force. When spun rapidly, lighter particles stay at the top and heavier particle go to the bottom during centrifugation, make the double emulsion nanoparticle that have been encapsulated should be heavier and stay at the bottom of the tube.

3.7 Collect the Pellet

The result from the centrifugation separated into two layers of supernatant which is the layer of free rapamycin, colchicine and PVA with another layer of pellet at the bottom of the double emulsion nanoparticles.

3.8 Store the pellet

Figure 15. Store the pellet in 5ml MQ

Figure 15 shows that, after getting the pellet of double emulsion nanoparticles, store the pellet in the MQ water at 4^0C condition to maintain the properties of the product.

3.9 Standard Curve

The standard curve of Rapamycin and Colchicine is used as a standard to find the unknown concentration of the nanoparticle after synthesized to measure the %encapsulation efficiency and % drug loading. For Rapamycin, use 1 mg of the drug dissolve in 1ml DMSO and from the value of the concentration the dilution times that suitable are 50x 150x 200x 300x 400x respectively. For Colchicine using 1mg of the drug and 1mlof DMSO as a solvent, the dilution times suitable are 50x 100x 150x 200x 300x respectively. The difference between the dilution times is that when diluting colchicine to 400x the values measured is a negative value which is an unusable value, so we need to use the higher value of the concentration.

3.10 Measure the percent encapsulation efficiency and percent drug loading

Using NanoDrop OneC to measure the UV-Vis to observe the %EE and %DL.

3.11 Dynamic Light Scattering (DLS)

3.11.1 Assembling the LOW Conductivity Cell

1. Attach the O-ring to each electrode block
2. Insert the glass cell holder. Orient and align the surface of the glass cell so that the opening is flat against the surface of the cell block.
3. Insert the electrode block from the side opposite the protrusion in the cell holder, and screw in until fully tightened.
4. Tighten the other electrode block on the other side. Both electrode blocks are identical. There is no left versus right orientation.
5. Put the sample into the glass cell using pipette. The recommended usable volume range is 1.5-2.5 ml.
6. Remove any bubbles, foam and insert the cell cap. To ensure that there are no bubbles or foam below the Daifron plunger.
7. Place the assembled low conductivity cell into the particle analyzer. Observe the data measured from the analyzer.

3.12 Zeta Potential (DelsaNano Submicron Particle Size and Zeta Potential)

3.12.1 Assemble the Flow Cell

1. Install the sealing rubber to the gutter of the cell guide and insert the glass cell into the
   concave portion of the cell guide
2. Insert the cell guide (holding of the Flow Cell) into the cell holder firmly to the bottom of the cell holder, pushing the cell guides against the glass cell and fitting the trenches on the cell guides to the pins of the cell holder.
3. Insert the electrode into one of the cell guides and then set the clamping knob, turning it clockwise.
4. Repeat steps 1-4 for the opposite side.
5. Set the luer fitting to the opening of the Flow Cell.
6. Turn the luer fitting clockwise to tighten it.
7. Fill the cell with sample solution.
8. Confirm that there are no bubbles in the glass cell and between the cell holder and the glass cell.
9. Set the cell stopper and turn it counterclockwise, pushing lightly until it stops.
10. Place the assembled flow cell inside the particle analyzer, then observe the data measured from the analyzer.

CHAPTER 4
EXPERIMENTAL RESULT AND DISCUSSION

In this chapter, presented the result of the percent of encapsulation efficiency and drug loading of the single emulsion and double emulsion nanoparticles from the pellet of the product created using NanoDrop one C for UV-Vis observation, the overall result obtained presented as bar charts compare with each conditions. Also, the DLS that commonly used to analyze and determine the distribution of molecules and particles with sizes of nanometer and Zeta potential to represent the surface of the nanoparticles synthesized.

4.1 The standard curve of Rapamycin and Colchicine

4.1.1 Standard Curve of Rapamycin

The result of the Standard Curve of the Rapamycin for the linear equation for further calculation of the encapsulation efficiency of the drug.

(a)

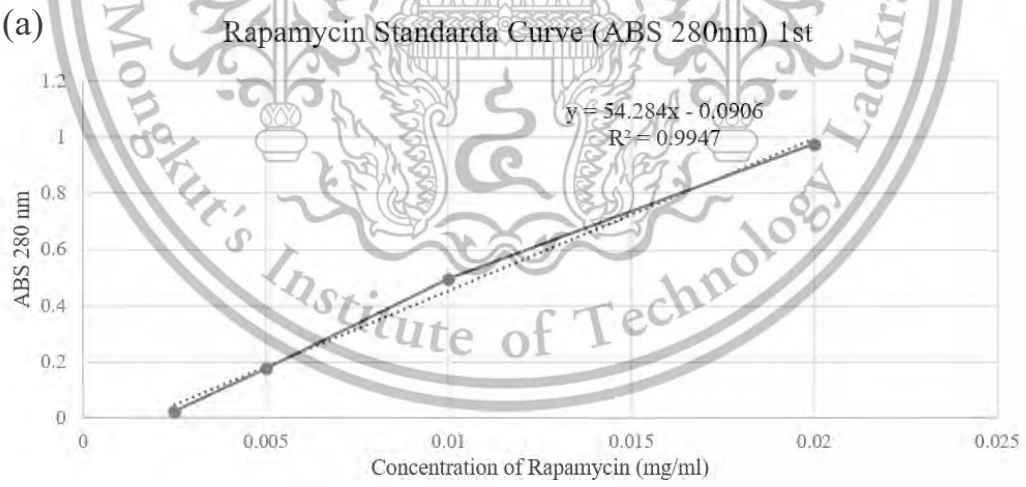

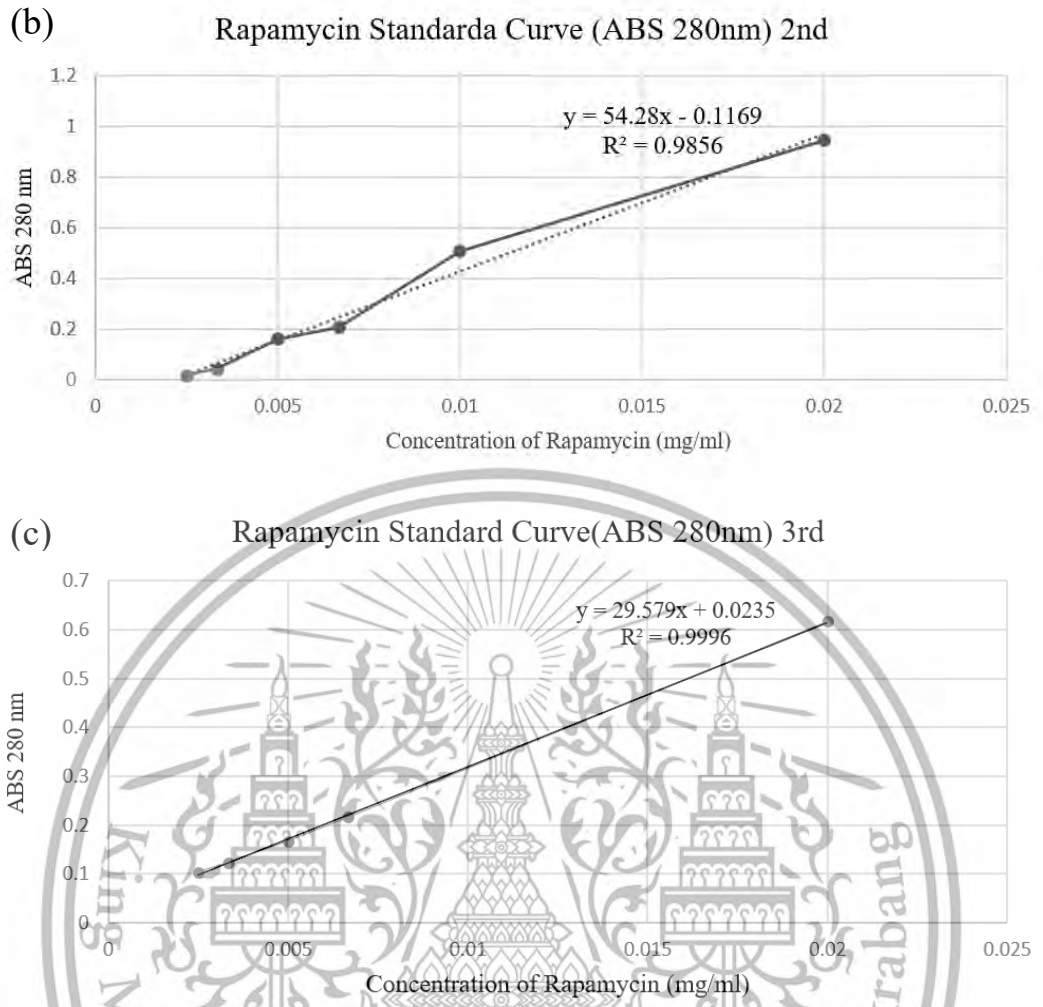

Figure 16. Rapamycin Standard Curve (a) 1st attempt (b) 2nd attempt (c) 3rd attempt

Figure 16 shows the repeat three times for rapamycin standard curve based on the compared R^2 value, (a) 0.9947, (b) 0.9856, (c) 0.9996, then choose the standard curve that R^2 value closet to 1.

Table 1. Value of the Rapamycin concentration at the absorbance of 280nm for the standard curve

Rapamycin	Dilution times	Concentration(mg/ml)	ABS(280nm)
	50	0.02	0.61666667
	150	0.00667	0.21666667
	200	0.005	0.16666667
	300	0.00333	0.12333333
	400	0.0025	0.10333333

The R^2 value of the 3rd rapamycin standard curve is 0.9996 which is the closet to one and the value of the concentration, dilution times and the wavelength that use to calculated the R^2 value shown in the Table 1 so, the linear equation of the 3rd

rapamycin standard curve has been chosen for the purpose of calculate the unknown value(x) of the concentration of the drug for the % encapsulation test and % drug loading test.

4.1.2 Standard Curve of Colchicine

Figure 17 shows the result of the Standard Curve of the Colchicine for the linear equation for further calculation of the percent encapsulation efficiency and percent drug loading of the drug.

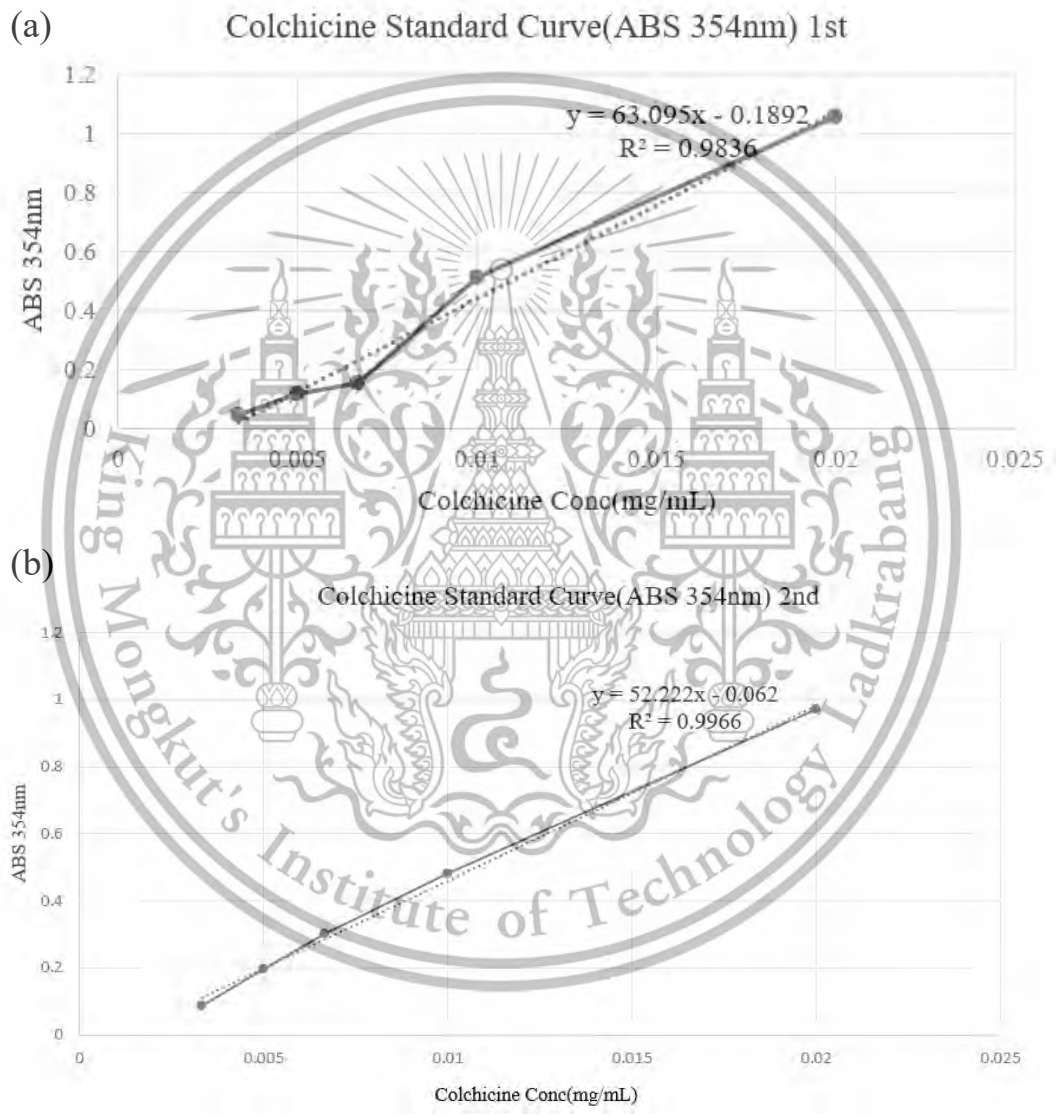

Figure 17. Standard curve of the Colchicine (a) 1st attempt (b) 2nd attempt

Figure 17 shows the repeat two times for rapamycin standard curve based on the compared R^2 value, (a) 0.9836, (b) 0.9966, then choose the standard curve that R^2 value closet to 1.

Table 2. Value of the Colchicine concentration at the absorbance of 280nm for the standard curve

Colchicine	Dilution times	Concentration(mg/ml)	ABS(280nm)
	50	0.02	0.97
	100	0.01	0.483333
	150	0.00667	0.303333
	200	0.005	0.196667
	300	0.00333	0.086667

The R^2 value of the 2nd rapamycin standard curve is 0.9966 which is the closest to one and the value of the concentration, dilution times and the wavelength that is used to calculate the R^2 value as shown in the Table 2. The linear equation of the 2nd rapamycin standard curve has been chosen for the purpose of calculating the unknown value (x) of the concentration of the drug for the % encapsulation test and % drug loading test.

4.2 The Result of Single Emulsion Nanoparticles of PLGA loaded with Rapamycin

In this experiment, using 1ml of pellet stored in MQ at 4C then centrifuge at 10k rpm for 10minutes, after that take the pellet to use. Dissolve the pellet of the nanoparticle using DMSO as a solvent. The concentration of the drug should be lower than 1 and not a negative value, so we could dilute it to be in an optimal concentration depending on the concentration at 1x Dilution time by using NanoDrop OneC with 4-5 µl of the sample then repeat 3 times and use the average value, as shown in the Table 3 and Table 4.

4.2.1 Result of Single Emulsion Nanoparticles of PLGA loaded with Rapamycin

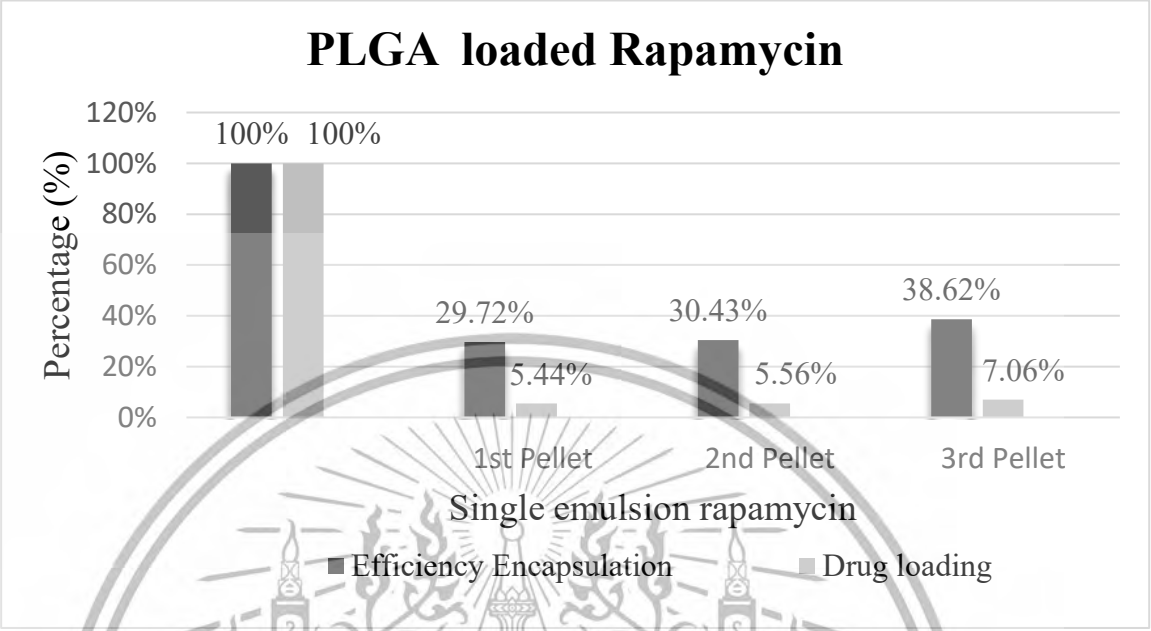

Figure 18. Graph of the % encapsulation efficiency and % drug loading of Single emulsion PLGA loaded with Rapamycin

According to Figure 18, the graph of the % Encapsulation Efficiency and % Drug loading of PLGA loaded with Rapamycin. The values of % Encapsulation Efficiency and % drug loading for 1st pellet are 29.72%, 5.44% and 30.43%, 5.56% for 2nd pellet and 38.62%, 7.06% for 3rd pellet respectively.

Table 3. Compare the results of Rapamycin %EE and %DL of single emulsion PLGA loaded with Rapamycin

Sample	Weight of the drug after Synthesis(mg)	EE(%)	DL(%)
1st Rapamycin Pellet	5.44	29.72	5.44
2nd Rapamycin Pellet	5.56	30.43	5.57
3rd Rapamycin Pellet	7.06	38.62	7.06
Mean	6.02 ± 0.9	32.92 ± 4.9	6.02 ± 0.9

Table 3 compares the values of the weight of the drug after synthesized, % Encapsulation efficiency, Drug loading of the Sample 1 to 3 of PLGA loaded Rapamycin and calculate the mean value.

4.3 The Results of Double Emulsion Nanoparticles of PLGA loaded with Rapamycin and Colchicine

4.3.1 The Result of % Encapsulation Efficiency and % Drug Loading of Rapamycin from Double Emulsion nanoparticle of PLGA loaded with Rapamycin and Colchicine

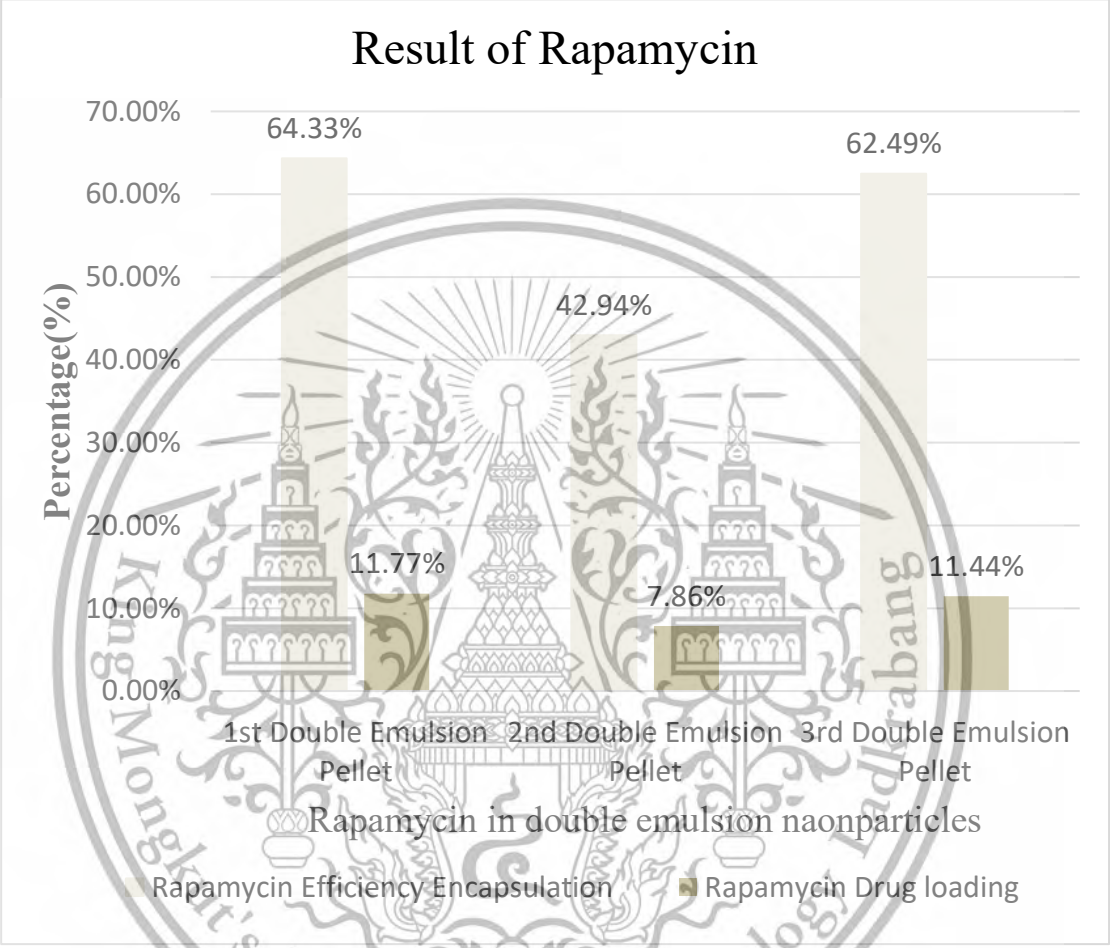

Figure 19. Graph Results of % Encapsulation Efficiency and % Drug Loading of Rapamycin from the Double Emulsion Nanoparticles of PLGA loaded with Rapamycin and Colchicine

Figure 19 shows, the result of the % encapsulation efficiency and % drug loading using NanoDrop OneC the result from the 1st attempt is 64.33% for encapsulation efficiency test and 11.77% for drug loading, for the 2nd attempt is 42.94% for encapsulation efficiency test and 7.86% for drug loading test and for 3rd attempt is 62.49% for encapsulation efficiency test and 11.24% for drug loading test.

Table 4. Compare the results of Rapamycin %EE and %DL of Double Emulsion PLGA loaded with Rapamycin and Colchicine

Sample	Weight of the drug after Synthesis(mg)	EE(%)	DL(%)
1st Double Emulsion Rapamycin Pellet	11.774	64.336	11.773
2nd Double Emulsion Rapamycin Pellet	7.858	42.944	7.858
3rd Double Emulsion Rapamycin Pellet	11.435	62.489	11.435
Mean	10.356 ± 2.17	56.589 ± 11.85	10.355 ± 2.17

Table 4 compares the values of the weight of the drug after synthesized, % Encapsulation efficiency, Drug loading of the Sample 1 to 3 of Rapamycin in PLGA loaded with Rapamycin and Colchicine then, calculate the mean value.

4.3.2 The Result of % Encapsulation Efficiency and % Drug Loading of Colchicine from Double Emulsion nanoparticle of PLGA loaded with Rapamycin and Colchicine

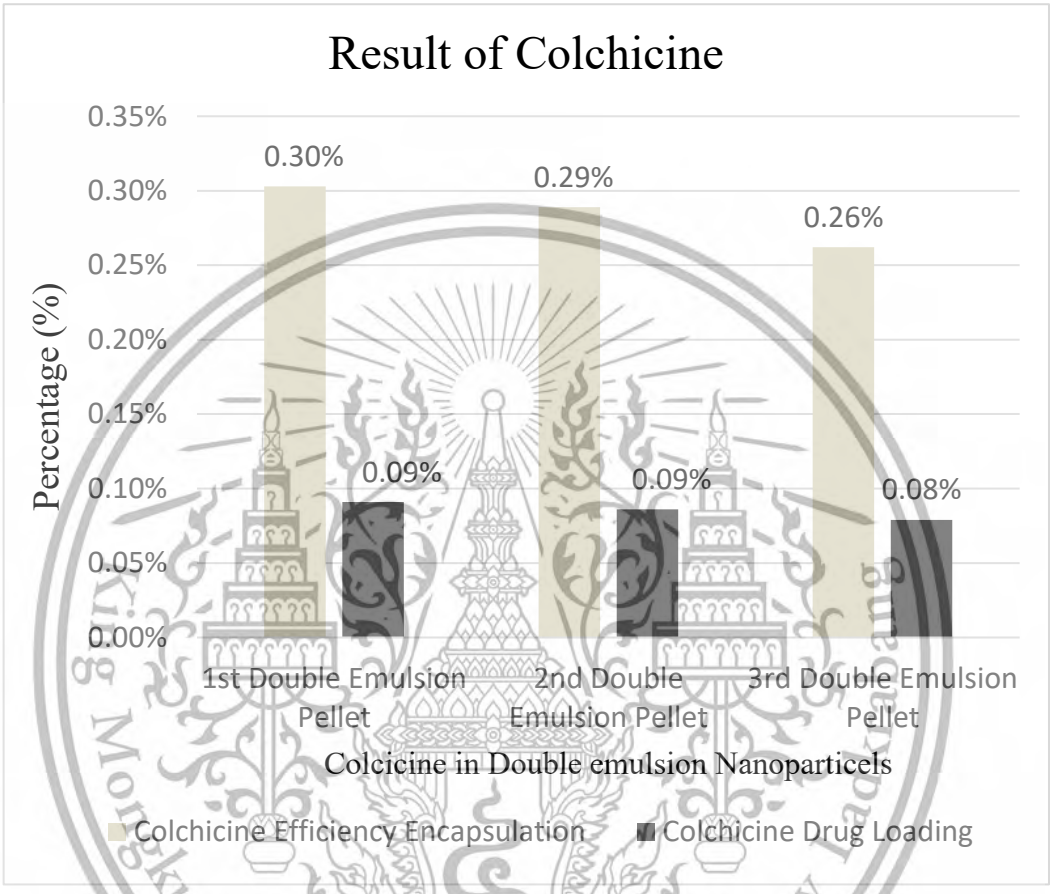

Figure 20. Graph Results of % Encapsulation Efficiency and % Drug Loading of Colchicine from the Double Emulsion Nanoparticles of PLGA loaded with Rapamycin and Colchicine

Figure 20 shows, the % encapsulation efficiency and % drug loading using NanoDrop OneC the result from the 1st attempt is 0.3% for encapsulation efficiency test and 0.09% for drug loading, for the 2nd attempt is 0.29% for encapsulation efficiency test and 0.09% for drug loading test and for 3rd attempt is 0.26% for encapsulation efficiency test and 0.08% for drug loading test, as shown in the figure 20.

Table 5. Compare the results of Colchicine %EE and %DL of Double Emulsion PLGA loaded with Rapamycin and Colchicine

Sample	Weight of the drug after Synthesis(mg)	EE(%)	DL(%)
1st Double Emulsion Colchicine Pellet	0.091	0.303	0.091
2nd Double Emulsion Colchicine Pellet	0.086	0.289	0.086
3rd Double Emulsion Colchicine Pellet	0.078	0.262	0.079
Mean	0.085 ± 0.0065	0.285 ± 0.021	0.085 ± 0.006

Table 5 compares the values of the weight of the drug after synthesized, % Encapsulation efficiency, Drug loading of the Sample 1 to 3 of PLGA loaded Rapamycin and calculates the mean value.

4.4 Zeta Potential result of PLGA nanoparticle, Single Emulsion Nanoparticle of PLGA loaded with Rapamycin, Double Emulsion Nanoparticle of PLGA loaded with Rapamycin and Colchicine.

4.4.1 Zeta Potential value of PLGA nanoparticles

(A)

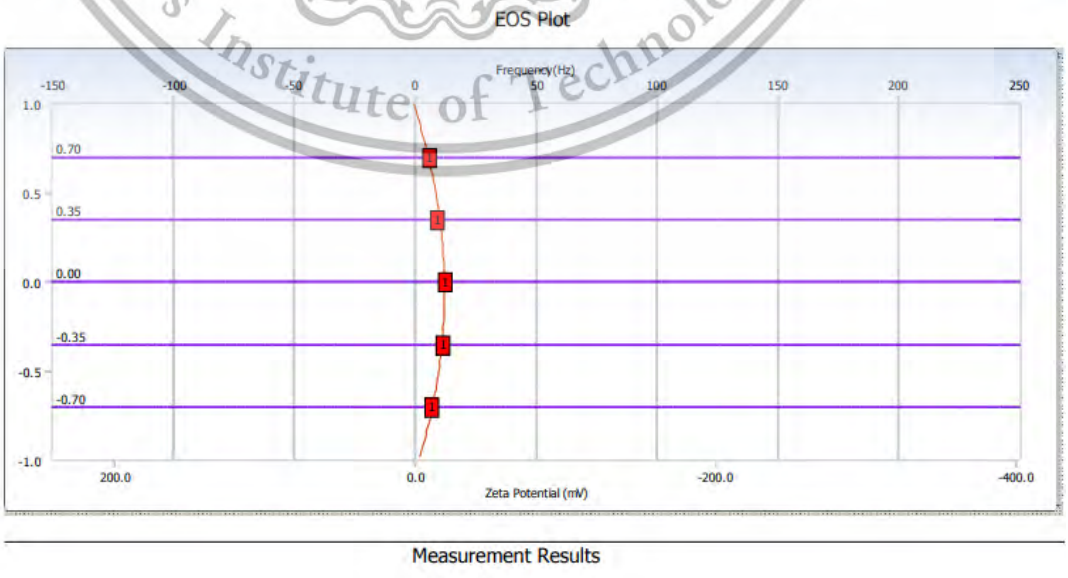

(B)

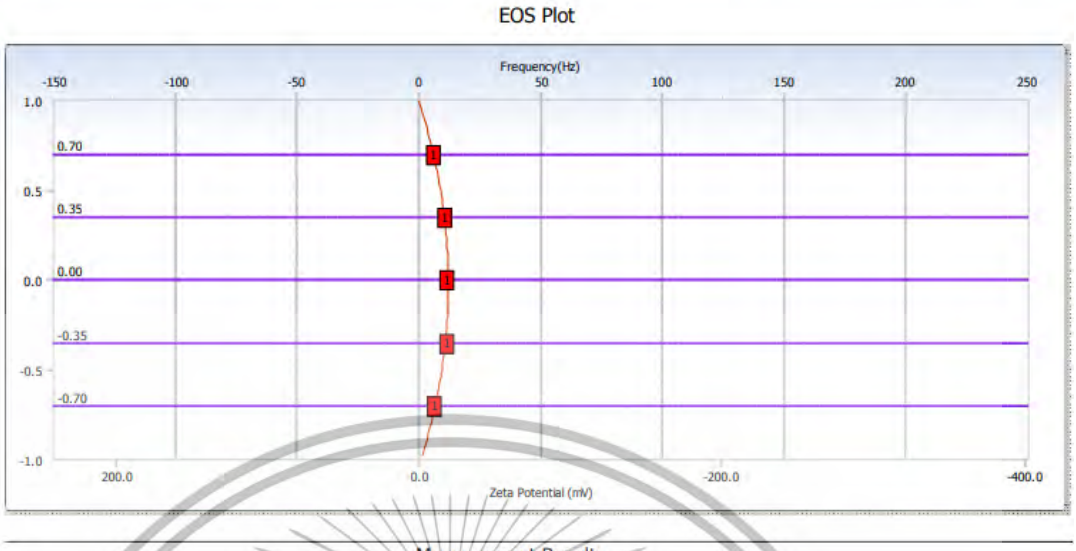

(C)

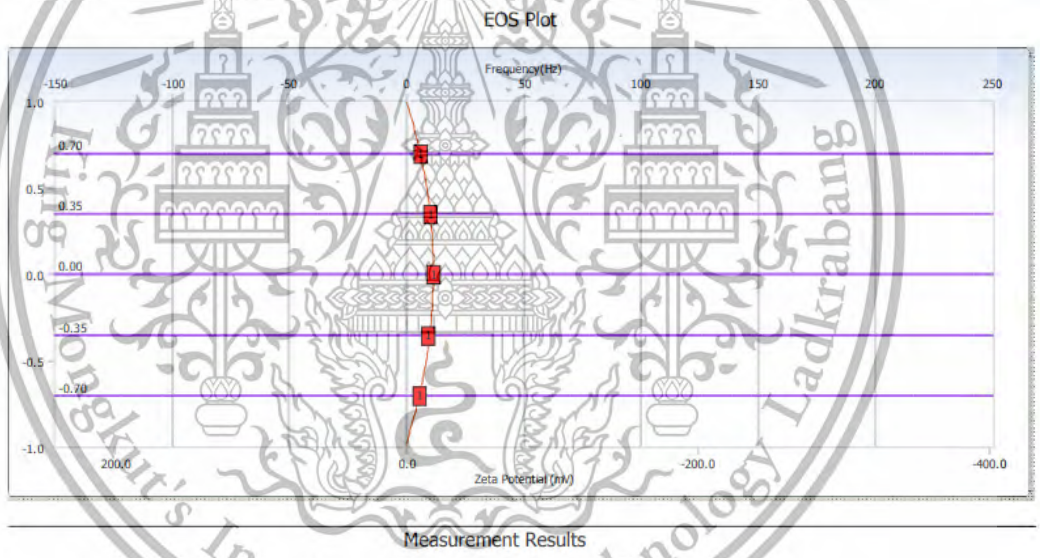

Figure 21. Zeta potential results of PLGA nanoparticles (A) 1st attempt (B) 2nd attempt (C) 3rd attempt

According to Figure 21 the average value of the zeta potential from attempts (A), (B), (C) of PLGA nanoparticles is -11.3733 ± 0.67 mV

4.4.2 Zeta Potential value of Single Emulsion nanoparticles loaded with Rapamycin

(A)

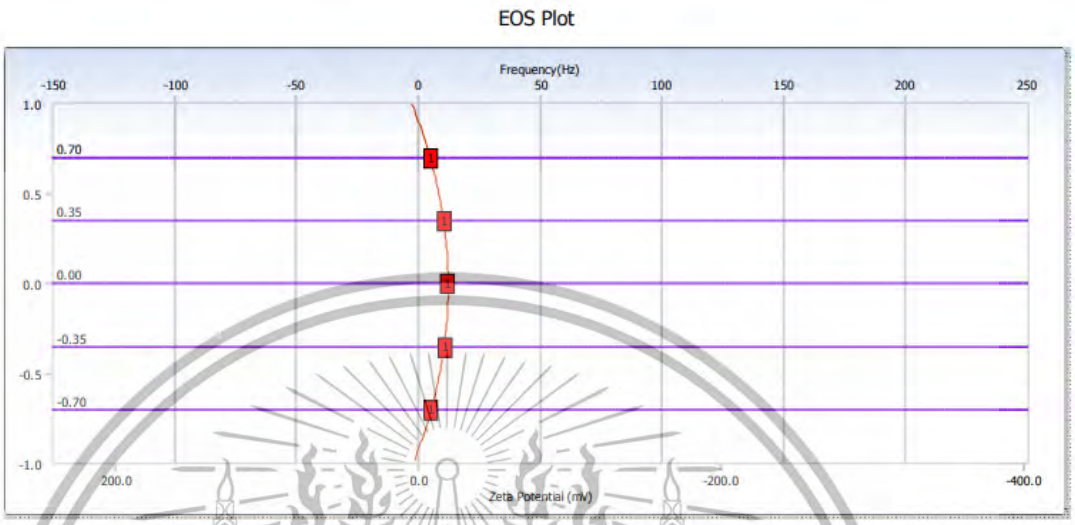

(B)

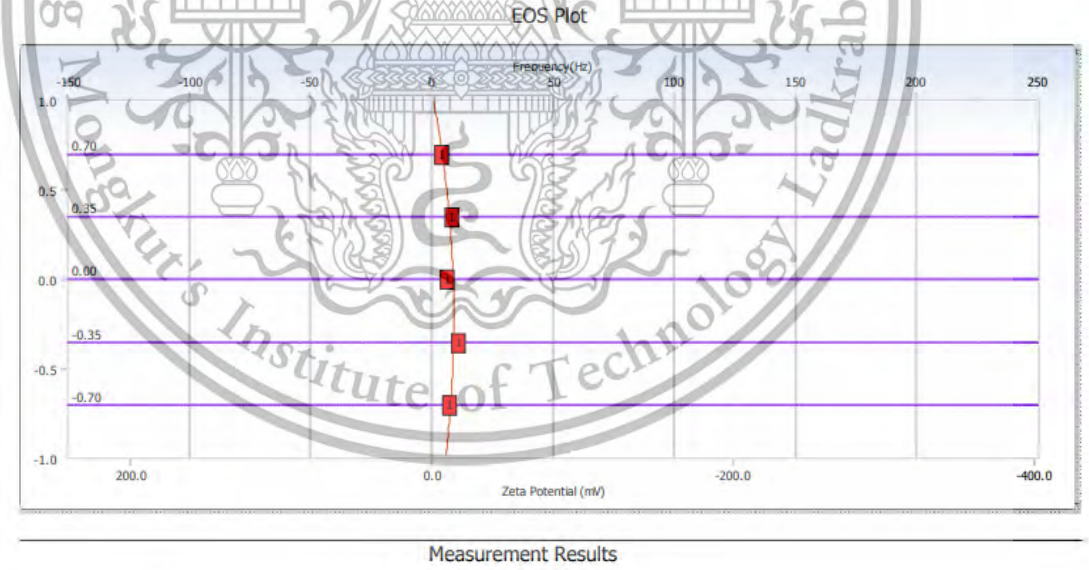

(C)

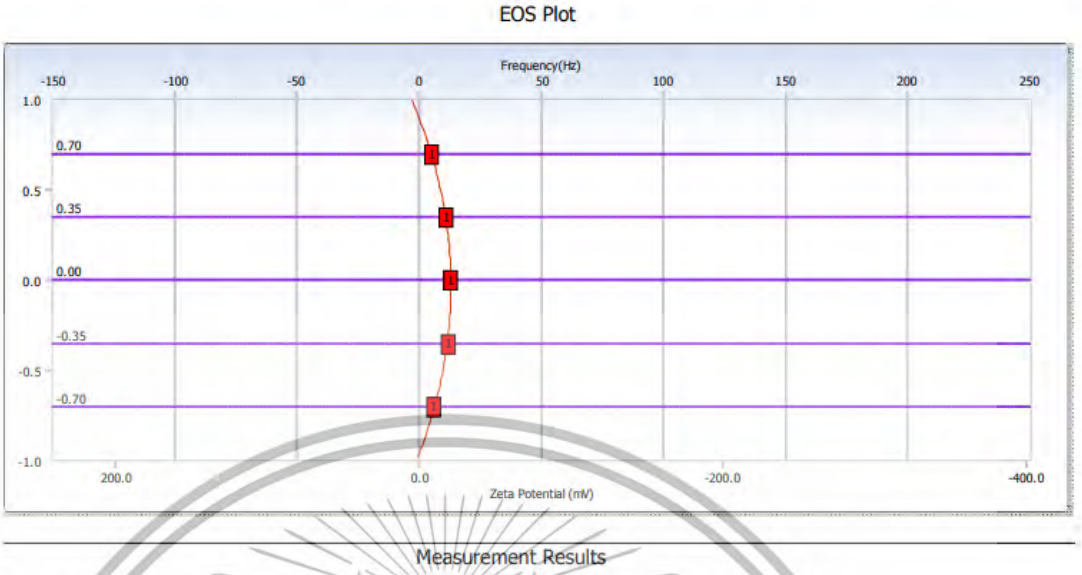

Figure 22. Zeta potential results of single emulsion nanoparticles of PLGA loaded with rapamycin (A) 1st attempt (B) 2nd attempt (C)

According to Figure 22 the average value of the zeta potential from attempts (A), (B), (C) of Single Emulsion nanoparticles loaded with Rapamycin is -10.5367 ± 0.50 mV

4.4.3 Zeta Potential value of Double Emulsion Nanoparticles of PLGA loaded with Rapamycin and Colchicine

(A)

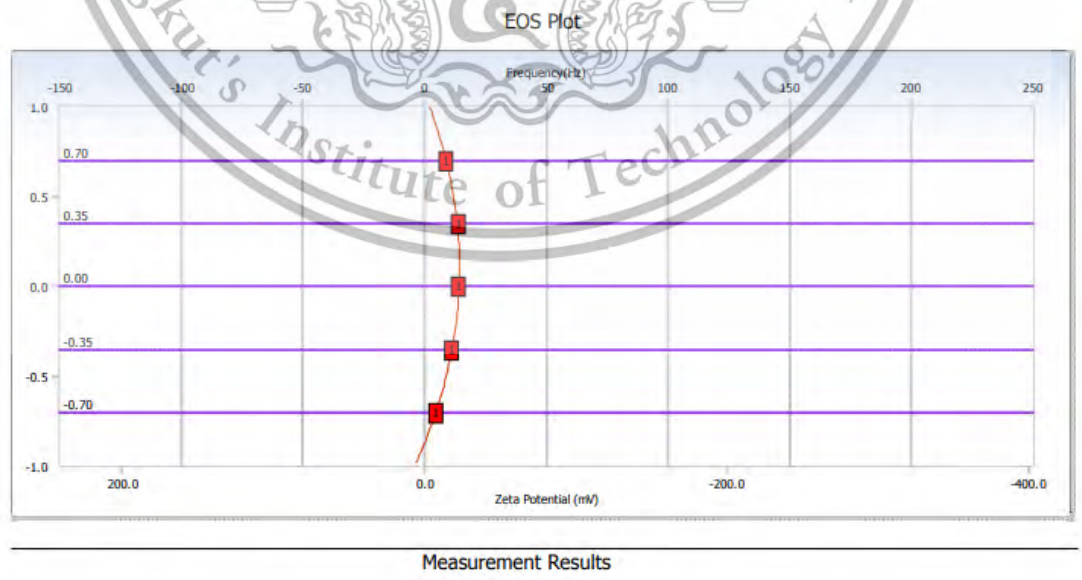

(B)

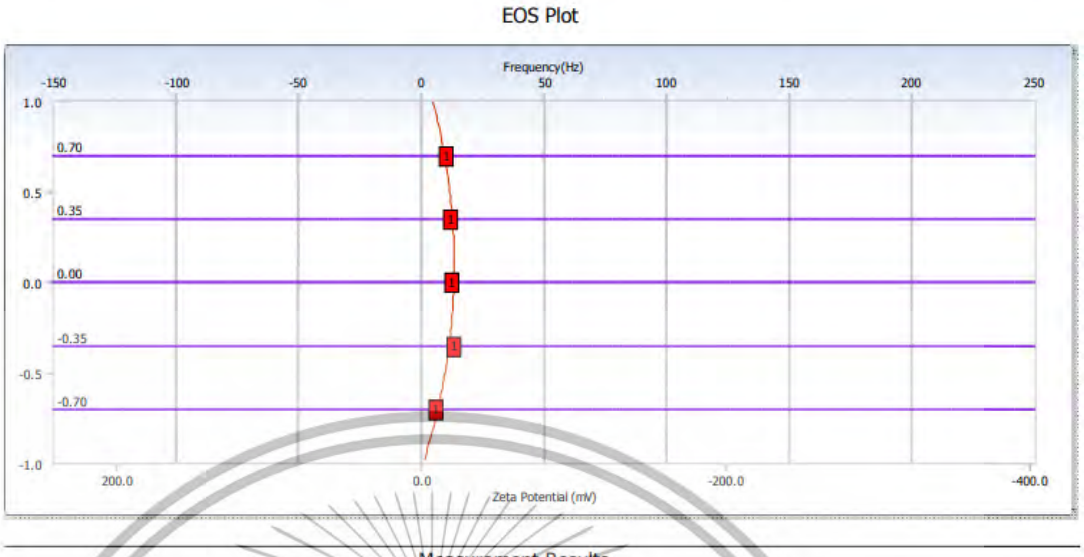

(C)

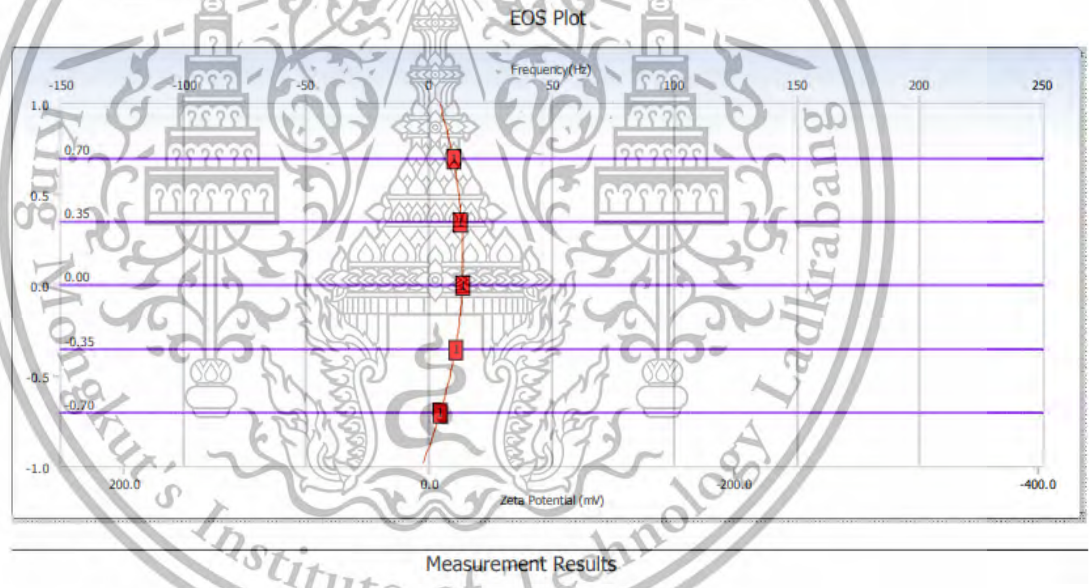

Figure 23. Zeta Potential value of Double Emulsion Nanoparticles of PLGA loaded with Rapamycin and Colchicine (A) 1st attempt (B) 2nd attempt (C)

According to Figure 23 the average value of the zeta potential from attempts (A), (B), (C) of PLGA loaded with Rapamycin and Colchicine nanoparticles is -13.5233 ± 0.88 mV

4.5 Discussion

4.5.1 Standard Curve

4.5.1.1 Standard Curve of Rapamycin

We conducted a series of three attempts to establish standard curve for rapamycin, using 2mg of rapamycin dissolved in DMSO as the solvent, with measurements taken via UV-Vis spectroscopy at the wavelength of 280 nm. The outcomes of these three attempts, During the first and second attempts, the linear equations are $y = 54.284x – 0.0906$ and $y = 54.28x – 0.1169$ with R^2 values of 0.9947 and 0.9856 respectively. On the third attempt, obtained a linear equation of $y = 29.579x + 0.0235$ and R^2 of 0.9996, as shown in Figure 16. This value is very close to 1, indicating that of the three attempts, the third attempt produces the most suitable standard equation. This equation can be used as the standard to determine the unknown concentration values of both single emulsion and double emulsion samples in order to calculate the percent encapsulation efficiency and percent drug loading of the product.

4.5.1.2 Standard Curve of Colchicine

For colchicine standard curve, two attempts were made. As the first and second attempts the data for the linear equation are $y = 63.095 – 0.1892$ for first attempt and $y =52.222x – 0.062$ for second attempt with R^2 value of these attempts are represented as 0.9836 and 0.9966 respectively, as shown in the figure 17. It is evident that the second attempts resulted in R^2 of the second attempt offers better accuracy for calculating the unknown concentration of the drug in the sample.

4.5.2 The Result of Single Emulsion Nanoparticles of PLGA loaded with Rapamycin

According to the remaining volume after removing the DCM the remaining be around 8-9 ml from the total of 1ml EtOH to dissolve rapamycin, 2.5ml of DCM for PLGA, and 10ml of PVA to encapsulate the drug creating a single emulsion nanoparticle which is the total of 13.5ml. We can say that the difference in the remaining volume of the product after removing DCM is the remaining itself, according to result the final product that has a higher remaining volume after removing the DCM tends to have a lower percent encapsulation efficiency and percent drug loading as remaining DCM is a solvent that can affect and dissolve the single emulsion nanoparticle pellet after centrifuged lead to a lower single emulsion nanoparticle remaining in the product.

4.5.3 The Results of Double Emulsion Nanoparticles of PLGA loaded with Rapamycin and Colchicine

4.5.3.1 The Result of % Encapsulation Efficiency and % Drug Loading of Rapamycin from Double Emulsion nanoparticle of PLGA loaded with Rapamycin and Colchicine

For double emulsion nanoparticle the total volume of the sample before removing DCM is 16 ml of 2.5ml of EtAC to dissolve Colchicine and PLGA, 1 ml EtOH to dissolve Rapamycin and 2.5ml of DCM to dissolve PLGA for Rapamycin, then the remaining volume after using vacuum pump to remove solvent is around 8-9 ml same as the single emulsion nanoparticle after removing the solvent. The difference is that during the process of removing DCM and other solvent the size of the bubble is smaller until after 10 minutes the size of the bubble start to increase to the same size of the bubble in the single emulsion nanoparticles. The volume of the product after removing the DCM and other also affect the percent encapsulation efficiency and percent drug loading as the higher the remaining the lower the encapsulation efficiency, the remaining volume of the product after removing DCM and other solvent have a volume of 8-8.5 ml, which mean that we removing higher amount of DCM make the pellet after centrifuge more clear that is from the pellet that we got is totally and the bottom of the centrifuge tube and not dissolve by the solvent and mix the free particle leading to a higher percentage of encapsulation efficiency from three attempts are 64.33%, 42.94%, 62.49% respectively and percentage of drug loading are 11.7%, 7.86%, 11.44% respectively, as shown in the figure 19.

4.5.3.2 The Result of % Encapsulation Efficiency and % Drug Loading of Colchicine from Double Emulsion nanoparticle of PLGA loaded with Rapamycin and Colchicine

The percentage encapsulation efficiency from three attempts are 0.303%, 0.29%, 0.26% respectively as shown in figure 20, which means that very low concentration of encapsulation efficiency and drug loading was obtained. Colchicine is a hydrophilic drug that is soluble in water, while PLGA is hydrophobic. The hydrophilic-hydrophobic mismatch can make it difficult for the drug to disperse within polymer during encapsulation. Hydrophilic drugs also have a higher likelihood of diffusing out of the hydrophobic polymer during encapsulation, reducing encapsulation efficiency.

4.5.4 Zeta Potential result of Encapsulated PLGA, Single Emulsion Nanoparticle of PLGA loaded with Rapamycin, Double Emulsion Nanoparticle of PLGA loaded with Rapamycin and Colchicine

4.5.4.1 Zeta Potential value of Encapsulated PLGA

The value of the zeta potential measured from the sample of encapsulated PLGA for three attempts are around -11.3733 ± 0.67 mV as shown in the figure 21, indicates the stability of a colloidal dispersion in this case are the nanoparticle that represented the ability of particles to repulse each other electrostatically. A zeta potential around -10mV indicates that there is some repulsion between the particles, which can help prevent the particles from aggregating or flocculating. However, the zeta potential values above ±30mV to ±60 mV suggest as a stable nanoparticle. So -10mV zeta potential indicates a somewhat stable dispersion nut could still be sensitive to changes depending on the environment, such as pH, ionic strength or substances that affect the surface charge.

4.5.4.2 Zeta Potential value of Single Emulsion Nanoparticles loaded with Rapamycin

The average values of zeta potential of single emulsion nanoparticles are 10.5367 ± 0.50 mV, as shown in the figure 22 indicating that there is some repulsion between the particles but low stability that can make the nanoparticles sensitive to the environmental factors.

4.5.4.3 Zeta Potential value of Double Emulsion Nanoparticles of PLGA loaded with Rapamycin and Colchicine.

For double emulsion nanoparticle the average values of zeta potential are -13.52 ± 0.88 mV, as shown in the figure 23 makes the nanoparticles have some repulsion between particles but low stability, which makes the nanoparticles sensitive to environmental factors.

CHAPTER 5
CONCLUSION

In this chapter will summarize the results from single to double emulsion nanoparticles. The equipment used for creating nanoparticles along with the devices used for characterization method and the results presented. Finally, suggestion on how this project for further improvement for better results in this research.

5.1 Conclusion

In the experiment of creating a standard curve for rapamycin the standard equation is $y = 29.579x + 0.0235$ with R^2 of 0.9996 from the third attempts of creating a standard curve as shown in the figure16, from 1-3 third attempt of 1mg rapamycin dissolve in 1ml DMSO before diluting, the different from the value due to the error during dilution process. For the process creating a single and double emulsion nanoparticle of rapamycin for single and both rapamycin and colchicine for double the using probe sonicator the condition are all the same for every nanoparticle created with 2 minutes timer, 60% amplitude, and with 30 seconds pulse and 20 seconds rest. According to the result from nanodrop one for the UV-VIS got the average value of the percent encapsulation efficiency and percent drug loading for the single emulsion nanoparticles of 32.92 ± 4.9% and 6.02 ± 0.9% respectively, as shown in the table 3 and for double emulsion nanoparticles of 56.589 ± 11.85% and 10.355 ± 2.17% for rapamycin and 0.285 ± 0.021 and 0.085 ± 0.006 for colchicine, as shown in the table 4 and table 5 respectively. The different in the result could be depends on the total volume of the product after the process of removing DCM, the higher final volume is remaining solvent in the product, after centrifugation the remain solvent make the pellet dissolve and mix with the free drug led to lower percent of encapsulation efficiency and percent drug loading. For characterization method of zeta potential, the average result from the PLGA nanoparticle, single emulsion nanoparticle of rapamycin and double emulsion nanoparticles of rapamycin and colchicine are -11.3733 ± 0.67 mV, -10.5367 ± 0.50 mV and -13.5233 ± 0.88 mV as shown in the figure 21, 22, 23 respectively. The results from zeta potential told us that the sample has a repulsion force between particles but as their values are low the particles will be less stable, mean that they'll sensitive to the environmental factor.

5.2 Suggestion

The suggestions for enhance the encapsulation efficiency of the double emulsion nanoparticles are trying to increase the time for removing DCM as there to ensure that the solvent completely remove from the product. For Dynamic Light Scattering (DLS) characterization method can be recommended to dilute the sample before measure to make the sample increase the probe sonication time for better agglomeration and more uniformly and smaller particle size.

REFERENCES

[1] A. Frank, M. Bonney, S. Bonney, L. Weitzel, M. Koeppen, and T. Eckle, "Myocardial Ischemia Reperfusion Injury:From Basic Science to Clinical Bedside," *Seminars in Cardiothoracic and Vascular Anesthesia,* vol. 16, no. 3, pp. 123-132, 2012, doi: 10.1177/1089253211436350.

[2] G. A. Roth *et al.*, "Global Burden of Cardiovascular Diseases and Risk Factors, 1990–2019: Update From the GBD 2019 Study," *Journal of the American College of Cardiology,* vol. 76, no. 25, pp. 2982-3021, 2020/12/22/ 2020, doi: https://doi.org/10.1016/j.jacc.2020.11.010.

[3] N. Garti and A. Aserin, "Double Emulsions," in *Encyclopedia of Colloid and Interface Science*, T. Tadros Ed. Berlin, Heidelberg: Springer Berlin Heidelberg, 2013, pp. 303-337.

[4] D. Chen, X. Liu, X. Lu, and J. Tian, "Nanoparticle drug delivery systems for synergistic delivery of tumor therapy," (in English), *Frontiers in Pharmacology,* Review vol. 14, 2023-February-16 2023, doi: 10.3389/fphar.2023.1111991.

[5] A. Das, F. N. Salloum, D. Durrant, R. Ockaili, and R. C. Kukreja, "Rapamycin protects against myocardial ischemia–reperfusion injury through JAK2–STAT3 signaling pathway," *Journal of Molecular and Cellular Cardiology,* vol. 53, no. 6, pp. 858-869, 2012/12/01/ 2012, doi: https://doi.org/10.1016/j.yjmcc.2012.09.007.

[6] R. A. Keates and G. B. Mason, "Inhibition of microtubule polymerization by the tubulin-colchicine complex: inhibition of spontaneous assembly," (in eng), *Can J Biochem,* vol. 59, no. 5, pp. 361-70, May 1981, doi: 10.1139/o81-050.

[7] H. K. Eltzschig and T. Eckle, "Ischemia and reperfusion—from mechanism to translation," *Nature medicine,* vol. 17, no. 11, pp. 1391-1401, 2011.

[8] A. R. Anzell, R. Maizy, K. Przyklenk, and T. H. Sanderson, "Mitochondrial quality control and disease: insights into ischemia-reperfusion injury," *Molecular neurobiology,* vol. 55, pp. 2547-2564, 2018.

[9] D. N. Granger and P. R. Kvietys, "Reperfusion injury and reactive oxygen species: The evolution of a concept," *Redox biology,* vol. 6, pp. 524-551, 2015.

[10] N. L. Halladin, "Oxidative and inflammatory biomarkers of ischemia and reperfusion injuries," *Dan Med J,* vol. 62, no. 4, p. B5054, 2015.

[11] G. Y. Chen and G. Nuñez, "Sterile inflammation: sensing and reacting to damage," *Nature Reviews Immunology,* vol. 10, no. 12, pp. 826-837, 2010.

[12] J.-i. Abe, C. P. Baines, and B. C. Berk, "Role of mitogen-activated protein kinases in ischemia and reperfusion injury: the good and the bad," *Circulation research,* vol. 86, no. 6, pp. 607-609, 2000.

[13] S. Ma, Y. Wang, Y. Chen, and F. Cao, "The role of the autophagy in myocardial ischemia/reperfusion injury," *Biochimica et Biophysica Acta (BBA)-Molecular Basis of Disease,* vol. 1852, no. 2, pp. 271-276, 2015.

[14] H. K. Makadia and S. J. Siegel, "Poly Lactic-co-Glycolic Acid (PLGA) as Biodegradable Controlled Drug Delivery Carrier," (in eng), *Polymers (Basel),* vol. 3, no. 3, pp. 1377-1397, Sep 1 2011, doi: 10.3390/polym3031377.

[15] Y. K. Sung and S. W. Kim, "Recent advances in polymeric drug delivery systems," *Biomaterials Research,* vol. 24, no. 1, p. 12, 2020/06/06 2020, doi: 10.1186/s40824-020-00190-7.

[16] T. Powers, "The origin story of rapamycin: systemic bias in biomedical research and cold war politics," (in eng), *Mol Biol Cell,* vol. 33, no. 13, Nov 1 2022, doi: 10.1091/mbc.E22-08-0377.

[17] B. Halford, "Rapamycin's secrets unearthed," *Chem. Eng. News,* vol. 94, pp. 26-30, 2016.
[18] Z. A. Knight *et al.*, "A pharmacological map of the PI3-K family defines a role for p110α in insulin signaling," *Cell,* vol. 125, no. 4, pp. 733-747, 2006.
[19] D.-H. Kim *et al.*, "GβL, a positive regulator of the rapamycin-sensitive pathway required for the nutrient-sensitive interaction between raptor and mTOR," *Molecular cell,* vol. 11, no. 4, pp. 895-904, 2003.
[20] H. E. Moon and S. H. Paek, "Mitochondrial Dysfunction in Parkinson's Disease," (in eng), *Exp Neurobiol,* vol. 24, no. 2, pp. 103-16, Jun 2015, doi: 10.5607/en.2015.24.2.103.
[21] D. A. Guertin and D. M. Sabatini, "An expanding role for mTOR in cancer," *Trends in molecular medicine,* vol. 11, no. 8, pp. 353-361, 2005.
[22] K. Hara *et al.*, "Raptor, a binding partner of target of rapamycin (TOR), mediates TOR action," *Cell,* vol. 110, no. 2, pp. 177-189, 2002.
[23] S. W. Ryter, S. M. Cloonan, and A. M. Choi, "Autophagy: a critical regulator of cellular metabolism and homeostasis," (in eng), *Mol Cells,* vol. 36, no. 1, pp. 7-16, Jul 2013, doi: 10.1007/s10059-013-0140-8.
[24] Y. Zhang, L. Liu, X. Hou, Z. Zhang, X. Zhou, and W. Gao, "Role of Autophagy Mediated by AMPK/DDiT4/mTOR Axis in HT22 Cells Under Oxygen and Glucose Deprivation/Reoxygenation," (in eng), *ACS Omega,* vol. 8, no. 10, pp. 9221-9229, Mar 14 2023, doi: 10.1021/acsomega.2c07280.
[25] C. Wei, H. Li, L. Han, L. Zhang, and X. Yang, "Activation of autophagy in ischemic postconditioning contributes to cardioprotective effects against ischemia/reperfusion injury in rat hearts," (in eng), *J Cardiovasc Pharmacol,* vol. 61, no. 5, pp. 416-22, May 2013, doi: 10.1097/FJC.0b013e318287d501.
[26] C. Chen-Scarabelli *et al.*, "The role and modulation of autophagy in experimental models of myocardial ischemia-reperfusion injury," (in eng), *J Geriatr Cardiol,* vol. 11, no. 4, pp. 338-48, Dec 2014, doi: 10.11909/j.issn.1671-5411.2014.01.009.
[27] D. Liu *et al.*, "Snapshot: Implications for mTOR in Aging-related Ischemia/Reperfusion Injury," (in eng), *Aging Dis,* vol. 10, no. 1, pp. 116-133, Feb 2019, doi: 10.14336/ad.2018.0501.
[28] B. Dasgeb, D. Kornreich, K. McGuinn, L. Okon, I. Brownell, and D. L. Sackett, "Colchicine: an ancient drug with novel applications," (in eng), *Br J Dermatol,* vol. 178, no. 2, pp. 350-356, Feb 2018, doi: 10.1111/bjd.15896.
[29] P. L. Geiger, "Ueber einige neue giftige organische Alkalien," *Annalen der Pharmacie,* vol. 7, no. 3, pp. 269-280, 1833.
[30] F. Martinon, V. Pétrilli, A. Mayor, A. Tardivel, and J. Tschopp, "Gout-associated uric acid crystals activate the NALP3 inflammasome," *Nature,* vol. 440, no. 7081, pp. 237-241, 2006.
[31] S. Kany, J. T. Vollrath, and B. Relja, "Cytokines in Inflammatory Disease," (in eng), *Int J Mol Sci,* vol. 20, no. 23, Nov 28 2019, doi: 10.3390/ijms20236008.
[32] D. D'Amario *et al.*, "Colchicine in ischemic heart disease: the good, the bad and the ugly," *Clinical Research in Cardiology,* vol. 110, no. 10, pp. 1531-1542, 2021/10/01 2021, doi: 10.1007/s00392-021-01828-9.
[33] A. Bonaventura, A. Vecchié, L. Dagna, F. Tangianu, A. Abbate, and F. Dentali, "Colchicine for COVID-19: targeting NLRP3 inflammasome to blunt hyperinflammation," (in eng), *Inflamm Res,* vol. 71, no. 3, pp. 293-307, Mar 2022, doi: 10.1007/s00011-022-01540-y.

[34] Y. Berkun *et al.*, "Pharmacokinetics and Colchicine in Pediatric and Adult Patients with Familial Mediterranean Fever," *International journal of immunopathology and pharmacology,* vol. 25, no. 4, pp. 1121-1130, 2012.
[35] D. Khanna *et al.*, "2012 American College of Rheumatology guidelines for management of gout. Part 2: therapy and antiinflammatory prophylaxis of acute gouty arthritis," *Arthritis care & research,* vol. 64, no. 10, pp. 1447-1461, 2012.
[36] L. Wilson, "Properties of colchicine binding protein from chick embryo brain. Interactions with vinca alkaloids and podophyllotoxin," *Biochemistry,* vol. 9, no. 25, pp. 4999-5007, 1970.
[37] N. Dalbeth, T. J. Lauterio, and H. R. Wolfe, "Mechanism of action of colchicine in the treatment of gout," *Clinical therapeutics,* vol. 36, no. 10, pp. 1465-1479, 2014.
[38] S. Pradhan, J. Hedberg, E. Blomberg, S. Wold, and I. Odnevall Wallinder, "Effect of sonication on particle dispersion, administered dose and metal release of non-functionalized, non-inert metal nanoparticles," *Journal of Nanoparticle Research,* vol. 18, no. 9, p. 285, 2016/09/22 2016, doi: 10.1007/s11051-016-3597-5.
[39] B. J. Berne and R. Pecora, *Dynamic light scattering: with applications to chemistry, biology, and physics*. Courier Corporation, 2000.
[40] S. Bhattacharjee, "DLS and zeta potential – What they are and what they are not?," *Journal of Controlled Release,* vol. 235, pp. 337-351, 2016/08/10/ 2016, doi: https://doi.org/10.1016/j.jconrel.2016.06.017.
[41] T. Ito, L. Sun, M. A. Bevan, and R. M. Crooks, "Comparison of nanoparticle size and electrophoretic mobility measurements using a carbon-nanotube-based coulter counter, dynamic light scattering, transmission electron microscopy, and phase analysis light scattering," *Langmuir,* vol. 20, no. 16, pp. 6940-6945, 2004.
[42] V. R. Patel and Y. Agrawal, "Nanosuspension: An approach to enhance solubility of drugs," *Journal of advanced pharmaceutical technology & research,* vol. 2, no. 2, p. 81, 2011.
[43] P. P. Pillai, B. Kowalczyk, W. J. Pudlo, and B. A. Grzybowski, "Electrostatic titrations reveal surface compositions of mixed, on-nanoparticle monolayers comprising positively and negatively charged ligands," *The Journal of Physical Chemistry C,* vol. 120, no. 7, pp. 4139-4144, 2016.